
Author Elina Pasanen

Title of thesis Electrostatic separation of Municipal Solid Waste Incineration Bottom Ash

Department Materials Science and Engineering

Professorship Mechanical Processing and Recycling **Code of professorship**
MT-46

Thesis supervisor Professor Kari Heiskanen

Thesis advisors/Thesis examiners M.Sc. Tero Ojanperä, M.Sc. Leena Tuominen

Date 13.10.2014**Number of pages** 96**Language**
English

Abstract

The recovery of copper and precious metals from fine (0-2 mm) non-ferrous fraction of municipal solid waste incineration (MSWI) bottom ash with a two-roll corona electrostatic separator was investigated. Corona electrostatic separator is typically used for separation of fine granular mixture with large differences in electrical conductivities of particles, f.e. mixture of plastic and metal. However, in this work the main objective was to find out if the selectivity of the corona electrostatic separator would be enough for the separation of metal fraction of bottom ash. Objective was also to investigate the effect of different equipment parameters on the separation results.

Experiments were carried out to test the effect of chosen parameters individually, and to test the effect of certain parameter combinations. Before the experiments, the test material was dried and screened to 0,28-2 mm. Separation results were analysed through the material distribution to different output fractions, through copper content of the output fractions and through precious metal content of product.

According to the separation results, corona electrostatic separator is not applicable for the separation of the test material. At best, only minor enrichment of copper and precious metals to product was achieved. Voltage and distance of output stream dividers from the roll electrode had the most significant effect on output mass fractions. The effect of all test parameters on copper and precious metal contents of product was relatively minor.

Keywords Electrostatic separation, bottom ash, municipal solid waste incineration

Tekijä Elina Pasanen		
Työn nimi Jätteenpolttolaitoksen pohjakuonan elektrostaattinen erotteleminen		
Laitos Materiaalitekniikka		
Professuuri Mekaaninen prosessi- ja kierrätystekniikka	Professuurikoodi MT-46	
Työn valvoja Professori Kari Heiskanen		
Työn ohjaajat/Työn tarkastajat DI Tero Ojanperä, DI Leena Tuominen		
Päivämäärä 13.10.2014	Sivumäärä 96	Kieli Englanti

Tiivistelmä

Tässä työssä tutkittiin kuparin ja jalometallien erottelemista yhdyskuntajätteen poltosta syntyvän pohjakuonan hienojakoisesta (0-2 mm) metallifraktiosta korona-elektrostaattisella rumpuerottimella. Kyseisen tyyppistä erotinta käytetään yleensä hienojakoisille materiaaliseoksille joiden partikkelien sähkönjohtavuudet poikkeavat toisistaan huomattavasti, kuten esimerkiksi muovi-metalli-seoksille. Työn päätavoitteena oli selvittää elektrostaattisen erottimen toimivuutta, säädettävyyttä ja selektiivisyyttä pohjakuonan metallifraktion rikastamiseen. Tavoitteena oli myös tutkia laitteiston eri parametrien vaikutusta erotustulokseen.

Työssä tutkittiin kokeellisesti sekä yksittäisten parametrien että valittujen parametriyhdistelmien vaikutusta erotukseen. Koemateriaali kuivattiin ja seulottiin raekokoon 0,28-2 mm. Erotustuloksia arvioitiin tutkimalla materiaalin jakautumista erotuksessa eri ulostulofraktioihin, analysoimalla fraktioiden kuparipitoisuuksia sekä analysoimalla tuotteen jalometallipitoisuuksia.

Erotustulosten mukaan elektrostaattisen erottimen selektiivisyys ei riitä koemateriaalin erottelemiseen, sillä parhaimmillaankin kuparin ja jalometallien rikastuminen tuotteeseen oli vähäistä. Koeparametreista jännitteellä ja materiaalivirran jakajien etäisyydellä rummuista oli suurin vaikutus eri fraktioiden massaosuuksiin. Yksikään koeparametri ei vaikuttanut merkittävästi fraktioiden kupari- ja jalometallipitoisuuksiin, vaan pitoisuuksissa oli havaittavissa ainoastaan pieniä muutoksia parametrien arvoja muutettaessa.

Avainsanat Elektrostaattinen erotus, pohjakuona, jätteenpoltto

Preface

This master's thesis has been made for Kuusakoski Oy in Kuusakoski Ekopark Lahti. Great thanks to Jyri Talja, the Kuusakoski Vice President of Technology, for giving me a chance to do my master's thesis among this subject, and to professor Kari Heiskanen for supervising my thesis. I found my work very interesting, especially the experimental part which provided variation and excitement to my work days. I wish the results of this thesis can be utilized in planning the becoming experiments with the electrostatic separator.

Warm thanks to my instructors Tero Ojanperä and Leena Tuominen for being so helpful and supportive throughout my work. Special thanks to Tero for your expertise and help in the theoretical part of my work, and for Leena for taking care I had everything I needed to complete the experiments successfully. I also cannot thank enough for Maria Lehtinen and Maiju Lehtinen, who made a huge work by analysing my samples. My gratitude belongs also to Timo Myllys and Jarmo Johansson who helped me with the practical issues related to the experiments.

Finally I would like to thank my family and friends for all the support during my work. Thank you for listening my work stories ad nauseam, empathising my joys and worries and giving valuable opinions and advice related to my work. I also want to express my great gratitude for my husband Asmo for patience, understanding and help especially during my busy work weeks, and for my twin sister Hanna for being always on my side in every issue and having such a positive approach to things.

Espoo 13.10.2014

Elina Pasanen

Table of contents

Introduction	2
I Literature review	4
1 Waste Incineration	4
1.1 Municipal solid waste incineration in Europe and in Finland	4
1.2 Waste incineration process	5
1.2.1 Theory and techniques	5
1.2.2 The function of waste incineration plant	6
1.2.3 Grate incineration technology	7
2 Residues from Waste Incineration	9
2.1 Bottom ash.....	10
2.1.1 Composition and particle size distribution	10
2.1.2 Treatment	12
2.1.3 Utilization	12
2.2 Fly ash and APC residue.....	13
2.2.1 Composition and particle size distribution	13
2.2.2 Treatment	15
2.2.3 Utilization	15
2.3 Boiler ash.....	16
2.3.1 Composition and particle size distribution	16
2.3.2 Treatment	18
2.3.3 Utilization	18
3 Electrostatic Separation.....	19
3.1 Corona electrostatic separation	20
3.1.1 Operating principle	20
3.1.2 Parameters affecting to separation efficiency	22
3.1.3 Applications	26
3.2 Plate-type electrostatic separation	26

3.3 Triboelectrostatic separation.....	28
II Experimental part	30
4 Test Equipment	30
4.1 Process and equipment	30
4.2 Electrostatic separator	32
5 Analysing Equipment.....	35
5.1 X-Ray Fluorescence (XRF) spectrometry	35
5.1.1 Disc mill.....	36
5.2 Inductively Coupled Plasma Optical Emission Spectrometry (ICP-OES) ...	36
5.3 Scanning Electron Microscope	37
6 Test Materials and Characterization	39
6.1 Material	39
6.1.1 Rotor impact mill.....	39
6.2 Characterization	40
6.2.1 Sieving	40
6.2.2 XRF and ICP analysis.....	42
6.2.3 SEM analysis	47
6.3 Theoretical value	50
7 Execution of Experiments	53
7.1 Preliminary experiments	54
7.2 Main experiments	55
7.3 Additional experiments	58
8 Results	61

8.1 Preliminary Experiments.....	61
8.1.1 Effect of Voltage.....	61
8.1.2 Effect of roll speed.....	62
8.1.3 Effect of corona electrode distance.....	64
8.1.4 Effect of static electrode distance	65
8.1.5 Effect of divider distance	66
8.2 Main experiments	67
8.2.1 Tests to improve product quality	67
8.2.2 Effect of corona electrodes on product's purity	70
8.2.3 Factor experiments.....	73
8.3 Additional experiments	78
8.3.1 Effect of feed rate	78
8.3.2 Effect of upper divider distance.....	81
8.3.3 Effect of moisture	83
8.3.4 Effect of dust.....	86
Conclusions	89
References	92

Abbreviations and acronyms

APC	Air Pollution Control
BANF	Non-ferrous fraction of Bottom Ash
CES	Corona Electrostatic Separator
ESP	Electrostatic Precipitator
ESS	Electrostatic Separator
F5	Fine (0-2 mm) non-ferrous fraction of bottom ash
F12	Fine (0-2 mm) non-ferrous fraction of bottom ash that has gone through rotor impact mill
HNF	Heavy Non-ferrous
ICP	Inductively Coupled Plasma spectrometry
MCA	Multi-Channel Analyser
MSW	Municipal Solid Waste
MSWI	Municipal Solid Waste Incineration
OES	Optical Emission Spectrometry
SEM	Scanning Electron Microscopy
XRF	X-ray Fluorescence spectrometry

Introduction

Background

Every year thousands of millions of tons of municipal solid waste (MSW) are produced worldwide, and waste management and utilization strategies are major concern in many countries. With incineration of municipal solid waste the volume of waste can be reduced by about 90 % and its mass by about 70 % while providing recovery of energy from waste to generate electricity. Residues from municipal solid waste incineration (MSWI) encompass bottom ash, boiler ash, fly ash and air pollution control (APC) residue generated at different points in the MSWI process. (Lam, C. et al. 2010)

Bottom ash covers approximately 80 % of MSWI residue (Chimenos, J.M. et al. 1999). Commonly the ash is disposed to landfill, or used as secondary building material, depending on the country in which it is produced (Lam, C. et al. 2010). Composition of the ash has been investigated a lot, and according to studies (Muchova L. et al. 2009, Chimenos, J.M. et al. 1999), the fine (0-2 mm) heavy non-ferrous (HNF) fraction of MSWI bottom ash contains considerable amounts of precious metals. However, according to literature review, efficient recovery methods for the valuable metals from fine fraction of bottom ash have been challenging to develop, and have not been implemented in large scale in industry.

Electrostatic separation describes technologies that utilize electrostatic forces to sort granular mixtures which consist of small particles having a large difference of electrical conductivity. Corona electrostatic separator, also called roll-type electrostatic separator, is typically used for sorting of mixtures containing metal and plastic particles, for example crushed waste printed circuit boards. It has proved to be very efficient in the separation of a mix of PVC and copper, recovering more than 94 % of the copper introduced into it, with purity higher than 99 %. (Tilmaline, A. et al. 2009)

Objective and structure of the thesis

The separation of copper and precious metals from fine (0-2 mm) non-ferrous fraction of MSWI bottom ash with corona electrostatic separator is investigated. Electrostatic separation is not typically used for this kind of material, probably because the

differences between particles' electrical conductivities may not be large enough for successful separation. However, the objective in this work is to find out if the selectivity of the separator would be high enough for this material to separate copper and precious metals from other particles, and investigate how the equipment parameters affect to separation results.

This thesis consists of two parts: literature review and experimental part. The first part of the literature review concentrates on waste incineration process and different residues of the process, and the second part to different electrostatic separation processes with main focus on corona electrostatic separation. Experimental part presents the test equipment, analyzing equipment and characterization of the test material, before introducing the experiments carried out and results of the experiments.

In this work, three kinds of experiments were carried out: preliminary experiments, main experiments and additional experiments. In preliminary experiments, the effect of separator's parameters on the separation results was investigated. In main experiments, the information received from preliminary experiments was utilized to improve the quality of the product and investigate further the effect of different variable combinations. In additional experiments, tests were carried out to investigate the effect of a few additional parameters on the separation. According to the results of the experiments, conclusions are made about the applicability of the corona electrostatic separator on the test material, as well as about the significance of the effect of test parameters on the separation.

I Literature review

1 Waste Incineration

1.1 Municipal solid waste incineration in Europe and in Finland

Municipal solid waste incineration (MSWI) in plants began in Europe's big cities at the end of 19th century. At first the purpose was only to improve the bad hygiene of cities, but when the amount of waste continued increasing the incineration came to be seen also as a way to dispose waste. Utilization of waste energy content became interesting when oil price started to increase at 1970's. This resulted to integration of waste incineration plants to district heating net, and electricity production in plants. (Vesanto, P. 2006)

At the present time the role of incineration in waste management varies a lot between different countries. In Denmark and Switzerland nearly all combustible waste is incinerated. The incineration rate is also high in Sweden and Netherlands, whereas in Spain, Finland, Poland and Hungary the rate is particularly small. At the moment waste incineration is increasing strongly in Europe because of limitations related to landfilling and due to invocation possibilities of the renewable energy included in waste. (Vesanto, P. 2006)

In Finland the only waste incineration plant for long time was the incineration plant in Oriketo in Turku. In 2007-2009 two other waste incineration plants were introduced in Riihimäki (Ekokem) and in Kotka, and in 2012 four other waste incineration plants were introduced in different parts of Finland. In addition there are four other power plants in construction and planning phase. The planned and introduced waste incineration plants are presented in Table 1. (Pöyry. 2012)

Table 1 Planned and introduced waste incineration plants in Finland. (Pöyry. 2012)

	Waste incineration capacity (t/a)	Commissioning	Production
Turku Energia	50 000	1975	district heat
Ekokem, waste incineration plant 1	160 000	2007	electricity and district heat
Kotkan Energia	100 000	2009	electricity, process steam and district heat
Lahti Energia	250 000	2012	electricity and district heat
Oulun energia	120 000	2012	electricity, process steam and district heat
Westenergy Oy	150 000	2012	electricity and district heat
Ekokem, waste incineration plant 2	160 000	2012	electricity and district heat
Vantaan Energia	340 000	2014	electricity and district heat
Tammervoima Oy	180 000	2014-2015	electricity and district heat
Turun Seudun Jätehuolto Oy	150 000	2016-2017	electricity and district heat
Keski-Savon Jätehuolto	130 000	-	EIA procedure started at the beginning of 2012
Waste incineration capacity in total	1 740 000		

1.2 Waste incineration process

1.2.1 Theory and techniques

Thermal treatment of municipal solid waste (MSW) is a chemical reaction between oxygen and the organic matter in the waste, in which a big part of the energy included in the waste transfers as a heat to the flue gases released in the combustion. The incineration process consists of three unit processes that happen partly simultaneously and cannot be totally separated to different phases. The three unit processes are combustion chamber, gas purification and energy recovery. The purpose of combustion chamber is to decompose organic compounds, produce slag (that can possibly be utilized) and minimize the volume of waste. Purification of the flue gas removes the harmful compounds and minimizes their concentrations, and energy recovery system recovers the energy. (Laine-Ylijoki, J. et al. 2005)

The techniques of waste thermal treatment are divided to three main types, according to the oxidation reaction. Incineration techniques aim to perfectly oxidizing combustion, whereas in gasification process the oxidation is only partial, and pyrolysis process happens in totally oxygen-free conditions. An incineration technique widely utilized in municipal solid waste incineration is grate incineration. (Laine-Ylijoki, J. et al. 2005)

1.2.2 The function of waste incineration plant

Figure 1 presents a schematic picture of waste incineration plant in Mustasaari in Finland which utilizes grate incineration to produce electricity and district heat from municipal solid waste.

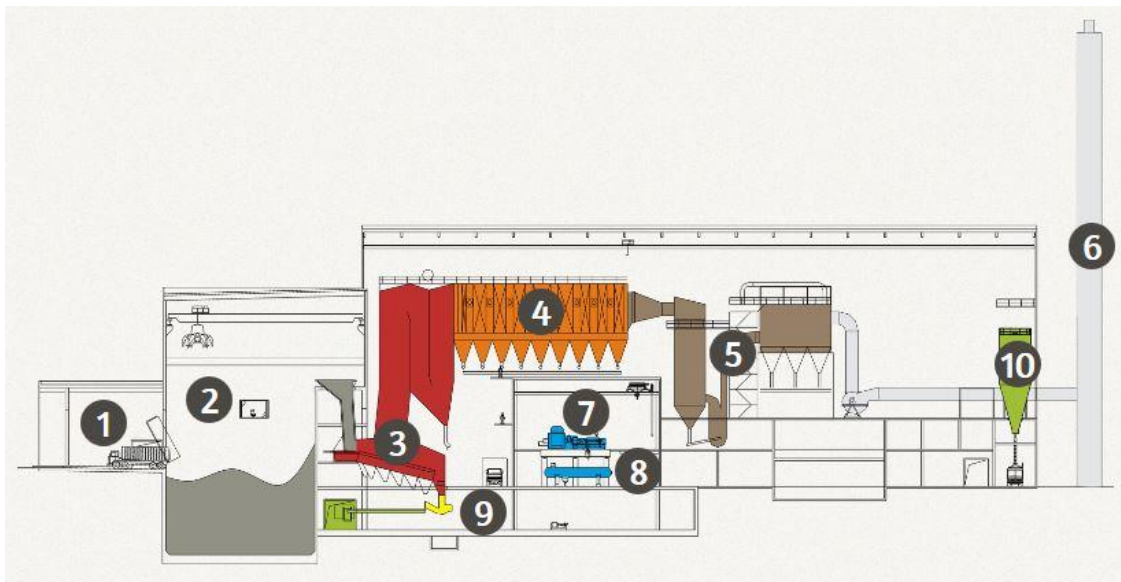


Figure 1 A schematic picture of Westenergy's waste incineration plant in Mustasaari in Finland (Westenergy. 2014)

Waste trucks drive to a reception hall (1) and empty their fuel load to a bunker (2) which works as storage to the waste. From the bunker the waste is fed to a grate (3), on which the incineration process happens. The hot slag formed in the process, called bottom ash, drops below the grate (9), is cooled by water and transported to containers. Heat transfer from combustion gas to boiler water happens mainly in a boiler (4). Boiler's walls consist of tubes filled with water. The water is heated to steam, after which the steam is superheated to 400 °C in 40 bars' pressure and lead to a turbine (7). The superheated steam rotates the turbine, and generator transforms the kinetic energy to electricity. Below the turbine hall is district heat center (8), where heat energy of the

hot steam is shifted to the cold water of district heating net. At the same time the steam condensates back to water which is transported back to the boiler and heated again. After the boiler the combustion gases are purified from chemicals and contaminants (5) and lead to a chimney (6). Combustion gases' purification waste (air pollution control residue and fly ash) is stored in a silo, as well as boiler ash which has been removed from the heat transfer surfaces of the boiler (10). (Westenergy. 2014)

1.2.3 Grate incineration technology

Grate incineration is a basic technique for the incineration of solid waste. It is widely applied in MSW incineration plants and in Europe approximately 90 % of installations treating MSW use grates. The technique is suitable for non-homogenous and low-caloric waste and does not require any special pretreatment of raw material: it is sufficient to crush large objects and remove big metal pieces. The process endures rather well variation in moisture, heat value and ash content of the waste. (Jätelaitosyhdistys. 2014)

In Figure 2 is presented a schematic picture of grate incineration furnace.

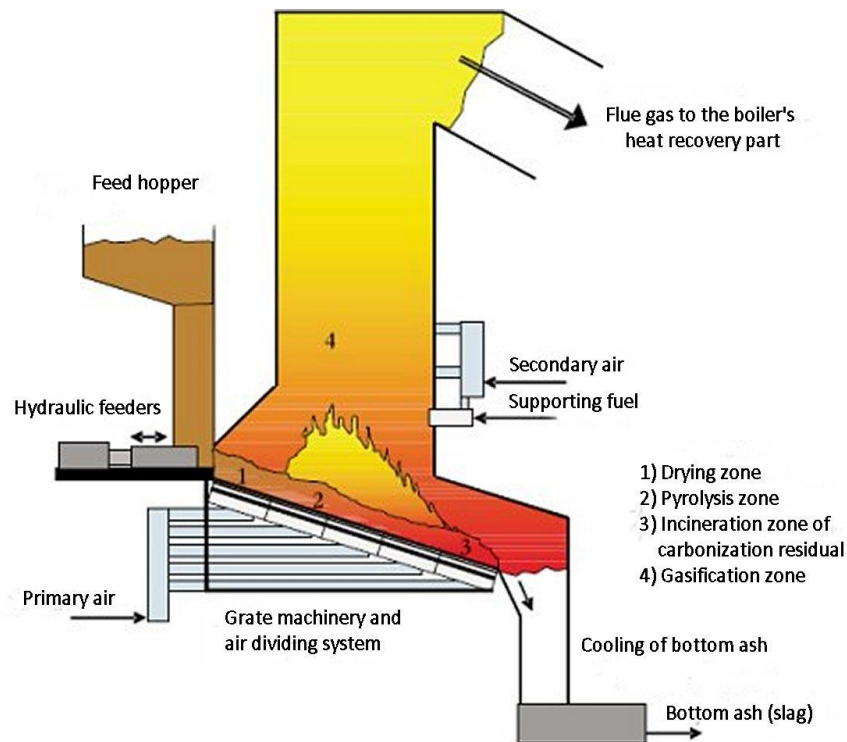


Figure 2 Principle of grate incineration furnace (Jätelaitosyhdistys. 2014)

In grate incineration the waste is fed with clamshell crane to a feed hopper, from which the waste is fed on to the grate with hydraulic feeders. Combustion chamber has the usual incineration zones of moist fuel: drying zone (1), pyrolysis zone (2), gasification zone (4) and finally the incineration zone of carbonization residual (3). New waste incineration plants typically have inclined grates that mix the waste during incineration process with different methods and on which the incineration can be controlled by adjusting the amount of air fed to different parts of the grate. (Jätelaitosyhdistys. 2014) “The primary air supply ensures the direct combustion of the waste, while the secondary air seeks to achieve turbulent mixing of the waste in order for the combustion to be complete.” Auxiliary firing systems are generally used to keep the temperature of the combustion gases high enough to accomplish complete combustion. (Waste Control. 2014) Coarse ash and unburned matter, such as metal pieces and stones, exit from the bottom of the grate to the plant’s bottom ash system. At the end of the combustion process the temperature is usually so high that the bottom ash is partly sintered and melted. (Jätelaitosyhdistys. 2014)

2 Residues from Waste Incineration

The main solid wastes formed in the waste incineration process are bottom ash, fly ash, air pollution control residue (APC) and mixes of these. (Kaartinen, T. et al. 2007) Bottom ash forms in the first stage of incineration process and consists primarily of coarse non-combustible materials and unburned organic matter. Fly ash consists of the fine particles still in the flue gases downstream of the heat recovery units. Air pollution control residues include the particulate matter captured in the gas purification phase. (Sabbas, T. et al. 2003) In addition small amounts of boiler ash is formed in the boiler that recovers energy from the combustion gas. (Kaartinen, T. et al. 2007) Grate siftings, which include relatively fine particles passing through the grate, are collected at the bottom of the combustion chamber and usually combined with bottom ash. (Sabbas, T. et al. 2003)

Figure 3 presents a process mass flow diagram which shows the generation of different types of ashes during the incineration process.

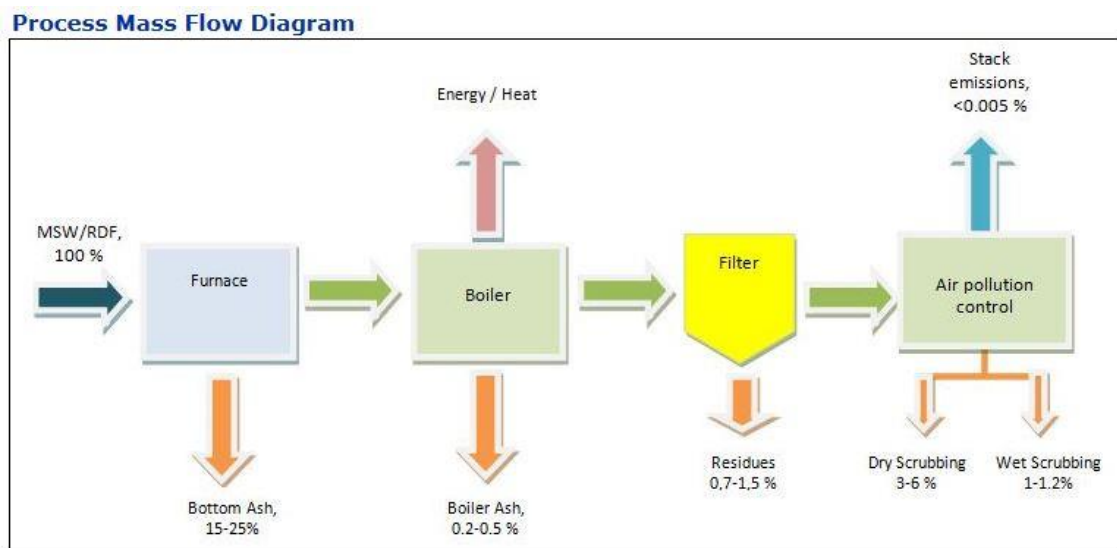


Figure 3 A process mass flow diagram of waste incineration plant (Waste Control. 2014)

In the following chapters bottom ash, fly ash, APC residue and boiler ash are presented more detailed. Fly ash and APC residue are reviewed together because they are often mixed with each other.

2.1 Bottom ash

2.1.1 Composition and particle size distribution

Bottom ash covers approximately 15-25 weight percent of the incinerated waste. (Waste Control. 2014) The relative proportion of substances in bottom ash depends on the composition of waste, volatility of substances and the type and function of the incineration boiler. 15-45 % of bottom ash is combustible material, such as metal, organic matter, glass and earth minerals (i.e. quartz), and 55-85 % is melting product consisting mainly of glass, siliceous minerals and oxide minerals (i.e. iron and lime). (Kaartinen, T. et al. 2007) Table 2 presents the typical element concentrations in bottom ash.

Table 2 Typical element concentrations in bottom ash (Kaartinen, T. et al. 2007)

Element	Concentration in bottom ash (mg/kg)
Al	21 900-72 800
As	0,12-189
Ba	400-3 000
Ca	370-123 000
Cd	0,3-70,5
Cl	800-4 190
Cr	23-3 170
Cu	190-8 240
Fe	4 120-150 000
Hg	0,02-7,75
Mg	400-26 000
Mo	2,5-276
Ni	7-4 280
Pb	98-13 700
Sb	10-432
Zn	613-7 770

From economic point of view the amount of precious metals and copper is especially interesting. Muchova et al. have studied precious metals in MSWI bottom ash and argue it contains economically significant levels of silver and gold, and with high prices of non-ferrous metals the separation of precious metals from the ash may be viable. They investigated bottom ashes from incinerators at Amsterdam and Ludwigshafen, and found out that Amsterdam's ash contains approximately 0.4 ppm of gold and 10 ppm of

silver. Ludwigshafen's ash contains similar amount of silver, but the sample was too small to give accurate values on gold content. (Muchova, L. et al. 2009) In Chandler's work the silver content in bottom ash world-wide is presented to be 0.29-36.9 ppm, the content of gold 0-20 ppm and the content of copper 190-8 240 ppm. (Chandler, A. et al. 1997) Hjelmar et al. have listed the ranges of element compositions of MSWI residues, and present the waste would contain 4.1-14 mg/kg silver and 900-4800 mg/kg copper. (Hjelmar, O. 1996)

Muchova et al. investigated the concentration of precious metals to size fractions of 0-2 mm, 2-6 mm and 6-20 mm. In the latter size fraction, which was handpicked, the number of precious metal particles was too small to give statistically significant results. In the size fractions of 0-2 mm heavy non-ferrous metal fraction (HNF) and 2-6 mm HNF the analysis showed the amount of gold to be approximately 100 ppm and the amount of silver 1500-4000 ppm. (Muchova, L. et al. 2009) In Chandler's work copper is presented to concentrate to size fraction of 0.4-2 mm with concentration of approximately 3000 mg/kg. (Chandler, A. et al. 1997) Allegrini et al. have investigated the resource recovery potential of MSWI bottom ashes, and charted rare earth metals' and precious metals' contents in different size fractions of bottom ash. According to their article the fine fraction (0-2 mm) of bottom ash would contain approximately 0.29 mg/kg of gold and 4800 mg/kg of copper. (Allegrini, E. et al. 2014)

Chimenos et al. have determined particle size distribution of MSWI bottom ash from faculties in Barcelona metropolitan area and in Tarragona metropolitan area in Spain in 1999. At the time of the investigations the two faculties handled mainly household waste, with a small input from commercial vendors. The results of the analysis showed that in both faculties up to 30 % of the bottom ash consists of particles bigger than 6 mm and up to 70 % of particles bigger than 3 mm. This fraction consists mostly of glass, synthetic ceramics and minerals, whereas magnetic metals are concentrated to the finest fraction and diamagnetic metals are randomly distributed to all size fractions. (Chimenos, J.M. et al. 1999) In Allegrini's article the fraction of fine material (0-2 mm) in bottom ash is presented to represent 37 % of MSWI bottom ash. (Allegrini, E. et al. 2014)

2.1.2 Treatment

To improve the characteristics of bottom ash and make its utilization more efficient several methods can be undertaken. In Europe mainly ageing, washing and separation of metals have been applied, whereas in Japan also vitrification technology is in use. (Laine-Ylijoki, J. et al. 2005)

Ageing of bottom ash results to several different reactions, for example carbonation, oxidation and various precipitation reactions, which help to improve the leaching properties. This improves the utilization possibilities of the ash because leachability mainly assesses i.e. the environmental quality of building materials to be applied on or in soil. Common ageing time varies from couple of months to half a year, but the process can be speeded up by controlling storage conditions and leading CO₂ through the material to speed up carbonization. (Steketee, J. et al. 1997)

Washing can be used to separate soluble and poorly soluble compounds from the matrix and from each other. (Laine-Ylijoki, J. et al. 2005) In the washing process, readily soluble components, i.e. bromide and chloride, can easily be removed with only little amount of water, whereas poorly soluble components, i.e. heavy metals, need large amounts of water and can usually still be removed only partially. To improve the solubility, treatment methods such as raising the temperature, the addition of complexers and pH correction can be undertaken. (Steketee, J. et al. 1997)

The purpose of metal separation is mainly to improve material recycling and reduce the total amount of ash. Traditionally only magnetic metals have been separated from bottom ash, but nowadays also non-magnetic metals are commonly removed. The quality of separated metal is usually good and it is suitable for recycling. (Laine-Ylijoki, J. et al. 2005)

2.1.3 Utilization

Bottom ash can be used in many excavation applications on behalf of its technical properties. The most typical applications are substructures and subgrade fillings of soil structure and superstructures in parking spaces, storage fields, sport fields and pedestrian and bicycle ways. (Kartinen, T. et al. 2010) Characteristics of treated bottom ash correspond to those of natural materials in many ways, and thus it can be

used to replace raw materials in for example cement production. In addition MSWI bottom ash has been used as raw material for the production of glasses, glass-ceramics and ceramics since it can replace part of the clay without pre-treatment, and as a partial replacement of commercial fertilizers since it contains acceptable amounts of phosphorous and potassium. It has also been used as an adsorbent to remove dye and heavy metals from wastewater. (Lam, C. et al. 2010)

2.2 Fly ash and APC residue

Fly ash means the fine particulate matter that is carried over from the combustor with the flue gases. It can be separated from flue gases by using wet, dry or semi-dry process. If wet process is used, fly ash is usually separated before the air pollution control, whereas in the case of dry and semi-dry processes fly ash usually goes through the air pollution control process and is separated together with other purification waste. Thus in the latter case fly ash ends up together with APC residues and separate fly ash fraction does not form. (ISWA. 2008)

2.2.1 Composition and particle size distribution

Fly ash and APC residues contain high concentrations of heavy metals, salts and organic micro-pollutants due to the volatilization and subsequent condensation as well as concentration phenomena acting during combustion (Sabbas, T. et al. 2003). The chemical characteristics of APC residues are strongly influenced by the separation process, the equipment used in it, reaction temperature and additives. (Kartinen, T. et al. 2007) Both the fly ash and APC residues are usually classified as hazardous waste due to the high concentrations of environmental hazardous elements. (Laine-Ylijoki, J. et al. 2005). In Finland the main components of the mix of fly ash and APC residue from waste incineration plant in Mustasaari are calcium(oxide) and chlorine. (Ekokem. 2014)

Table 3 presents the typical concentrations of important residue components in fly ash, in dry or semi-dry processed APC residue containing fly ash and in wet processed APC residue without fly ash. The last column contains the concentrations of metals and semi-metals analyzed from the annual collection of dry processed APC residue from Westenergy's waste incineration plant in Mustasaari.

Table 3 Typical element concentrations in fly ash, APC residue and mix of fly ash and APC residue (IAWG. 1997) and metal and semi-metal concentrations in Westenergy's waste incineration plant's APC+fly ash residue (Ekokem. 2014)

Element	Fly ash (ppm)	APC residue (ppm)	APC residue + fly ash (ppm)	Westenergy (APC residue + fly ash) (ppm)
Al	49 000-90 000	21 000-39 000	12 000-83 000	
As	37-320	41-210	18-530	43
Ba	330-3 100	55-1 600	51-14 000	
Ca	74 000-130 000	87 000-200 000	110 000-350 000	
Cd	50-450	150-1 400	140-300	140
Cl	29 000-210 000	17 000-51 000	62 000-380 000	
Cr	140-1 100	80-560	73-570	170
Cu	600-3 200	440-2 400	16-1 700	800
Fe	12 000-44 000	20 000-97 000	2 600-71 000	
Hg	0,7-30	2,2-2 300	0,1-51	16
K	22 000-62 000	810-8 600	5 900-40 000	
Mg	11 000-19 000	19 000-170 000	5 100-14 000	
Mn	800-1 900	5 000-12 000	200-900	
Mo	15-150	2-44	9-29	
Na	15 000-57 000	720-3 400	7 600-29 000	
Ni	60-260	20-310	19-710	21
Pb	5 300-26 000	3 300-22 000	2 500-10 000	2 100
S	11 000-45 000	2 700-6 000	1 400-25 000	
Sb	260-1 100	80-200	300-1 100	600
Si	95 000-210 000	78 000	36 000-120 000	
V	29-150	25-86	8-62	12
Zn	9 000-70 000	8 100-53 000	7 000-20 000	10 000

The particle size distribution of fly ash and APC residue is affected a lot by the separation processes. For example fly ash without acid gas cleaning residue contains generally a lower proportion of fine material than dry and semi-dry processed APC residues. Also the proportion of fine material in fabric filter residues is higher than in residues collected in electrostatic precipitators (ESPs), because fabric filters remove submicron size particles more efficiently than ESPs. For the sludge-like residues from wet scrubber APC processes it is not relevant to determine the particle size distribution. (Chandler, A. et al. 1997) According to the studies of Aubert et al. and Chandler et al, nearly all the fly ash and APC residue particles are smaller than 0,5 mm by diameter, 50

to 80 % of the particles are smaller than 0,1 mm and 30 to 60 percent are smaller than 0,01 mm. (Aubert, J.E. et al. 2006, Chandler, A. et al. 1997)

2.2.2 Treatment

In Europe the treatment of fly ash and APC residues aims primarily at minimizing the long-term solubility of heavy metals in disposal. The techniques used in the treatment of APC residues are based on solidification, thermal treatment, leaching and stabilization techniques and the combinations of them. The techniques differ from each other on how efficiently they improve the environmental properties and energy and raw material efficiency of the residues. (Laine-Ylijoki, J. et al. 2005) Many of the existing techniques have only been tested in lab or pilot scale and are not in commercial use. (ISWA. 2008)

Solidification and stabilization techniques have been developed especially for binding heavy metals. Available techniques are inter alia mixing of different materials, usage of hydraulic binders, combined washing and usage of hydraulic binders and usage of organic binders. Thermal treatment, containing melting and vitrification, improves the solubility characteristics of the residue and decomposes dioxins and furans. Leaching techniques are most commonly based on leaching of heavy metals and salts with acids. (Laine-Ylijoki, J. et al. 2005)

The mix of fly ash and APC residue from Westenergy's plant exceeds the limit values of hazardous waste on behalf of calcium chloride and zinc. To make the ash suitable for disposal it is stabilized and solidified. (Ekokem. 2014)

2.2.3 Utilization

Research and development activities related to APC residues have primarily focused on improving leaching properties of the residues rather than on techniques for recovery and utilization. Even though the interest into these aspects has risen significantly within the recent decade, there are only few commercially available recovery and utilization technologies on the market. One reason for this is the difficulty to achieve satisfactory technical quality for products based on APC residues and readily available virgin materials. (ISWA. 2008) Also the classification of APC residues as hazardous waste complicates the utilization of it.

However, some techniques for recovering certain substances from the residue, for example metals and salts, are in commercial use. The recovered components can be used as substitutes for the similar virgin material in a similar manner. APC residue could also be utilized in cement based applications, as a filler material (highway ramps, noise barriers etc.) and as a neutralizer for acidic waste materials. (ISWA. 2008) For example in Norway the waste treatment center in Langøya island receives and disposes hazardous non-organic waste (i.e. MSWI ashes) and uses it to neutralize ferrous sulfuric acid waste. (Laine-Ylijoki, J. et al. 2005) Aubert et al. have investigated the possibility to use treated fly ash in cement production and have got encouraging results. (Aubert, J.E. et al. 2006) Fly ash has also already been used as a substitute in filler material in asphalt production in The Netherlands (ISWA. 2008).

In Finland fly ash, APC residue and the mixes of them are usually classified as hazardous waste and disposed to the hazardous waste landfill. For example Ekokem which has investigated the fly ash and boiler ash from waste incineration plant in Mustasaari states that because of the soluble detrimental elements and the hazardous waste classification there is no utilization possibilities for the ashes. (Ekokem. 2014)

2.3 Boiler ash

Boiler ash consists of the coarse fraction of the particulate carried over by the flue gases from the combustion chamber and collected from the inner surfaces of boiler and economizer. (Sabbas, T. et al. 2003) It covers approximately 0.5 % of the input waste's weight and composes mainly of oxides, carbonates, sulfates, and chlorides. (Yang, Y. et al. 2008) Boiler ash is often mixed with fly ash and APC residue (Laine-Ylijoki, J. et al. 2005) or with bottom ash (Hjelmar, O. 1996), which is probably one reason for the difficulty to find scientific research about boiler ash.

2.3.1 Composition and particle size distribution

Ekokem has investigated the boiler ash from Mustasaari waste incineration plant and found out that the main components in the boiler ash were calcium oxide (approximately 30 %), silicon dioxide (approximately 25 %) and aluminium oxide (approximately 10 %). In addition boiler ash contained to some extent chlorine, sulphur and other oxides. (Ekokem. 2014) Yang et al. characterized the boiler ash from a Dutsch

MSW incineration plant with similar kinds of results. Table 4 presents the major elements of the boiler ash from the Dutch plant and Table 5 the metal and semi metal concentrations of the boiler ash from Mustasaari waste incineration plant.

Table 4 Major elements of the boiler ash from a Dutch MSW incineration plant (Yang, Y. et al. 2008)

Element	Concentration (wt%)
Ca	22.7
Si	12.2
S	4.62
K	5.99
Cl	11.1
Na	5.54
Al	3.98
Fe	2.44
Zn	2.89
Ti	1.79
Mg	1.42
P	0.83
Pb	0.64
F	0.93
Ba	0.22
Sb	0.22
Mn	0.1

Table 5 Metal and semi metal concentrations of the boiler ash from Mustasaari (Ekokem. 2014)

Element	Concentration (mg/kg)
Zn	8400
Pb	1000
Cu	630
Cr	570
Sb	450
Cd	50
V	49
As	48
Co	44
Hg	0.23

2.3.2 Treatment

Boiler ash is often classified as hazardous waste and requires treatment before disposal. In the Netherlands, cement solidification is generally used to reduce the leachability of contaminants out of the waste matrix. (Yang, Y. et al. 2008) In Finland the boiler ash from Mustasaari plant is also treated with cement stabilization and solidification. (Ekokem. 2014) However, by cementation or chemical treatment it is difficult to destroy or immobilize dioxins. In addition, alkali chlorides hinder hydration of cement. Vitrification is a technique that efficiently destroys organic and toxic compounds, immobilizes environmentally harmful elements and reduces the volume significantly. Disadvantages of the thermal processing are a secondary fly ash generation and high energy costs. (Yang, Y. et al. 2008) In vitrification process “residues are mixed with glass precursor materials and then combined at high temperatures into a single-phase amorphous, glassy product” (Sabbas, T. et al. 2003).

2.3.3 Utilization

In Finland boiler ash is generally treated and disposed to the hazardous waste landfills. As in the case of fly ash, according to Ekokem there are no utilization possibilities to boiler ash because of the hazardous waste classification and soluble detrimental elements. (Ekokem. 2014) Also in the article by Yang et al. the vitrification of boiler ash is investigated to improve the disposal possibilities of the ash: anything about the utilization possibilities is not mentioned. However, if the boiler ash is mixed with fly ash and/or APC residue or bottom ash as it often is, the utilization possibilities are likely to be similar as in the case of the ash fraction to which the boiler ash is mixed.

3 Electrostatic Separation

Electrostatic separation is mainly used for the dry separation of small particles having a large difference of electrical conductivity (Higashiyama, Y. et al. 1998). However, certain electrostatic separation methods can also be used to separate non-conductors with different surface properties, for example plastics (Wu, G. et al. 2013). Historically the technique has been developed for mineral beneficiation and for seed conditioning, but later it has been refocused on recovering metallic and insulating material from waste to conserve global resources. (Higashiyama, Y. et al. 1998)

Electrostatic separation technology provides many advantages compared to the other methods used for metal recovery, for example traditional fluid bed production line. It is simple, has low energy consumption and does not generate any wastewater. A lot of research has been done to optimize the separation process, since its efficiency is influenced by electrical, mechanical, material, and environmental factors. At present, electrostatic separation has been successfully applied in industrial scale and has proved to be efficient and environmental friendly separation technology. (Xue, M. et al. 2012)

Electrostatic separators consist of feeding, charging and sorting zones. A key factor in any separation is the charging of the particles, which is usually done by induction, corona or triboelectricity. The differences in particles' polarities and in amounts of charge the particles acquire affect to the separation capability. Induction and corona charging can be successfully used for particles having large difference in conductivities. In case there is no difference, tribocharging could be the option. (Higashiyama, Y. et al. 1998)

The following chapters present the operation of different electrostatic separators. Corona electrostatic separation is studied more detailed due to its relevance for this work, whereas plate-type separation and triboelectrostatic separation are presented only briefly.

3.1 Corona electrostatic separation

3.1.1 Operating principle

Corona electrostatic separation (CES) is a technique used to separate conductors from non-conductors. There are at least two kinds of charging equipment: rotational drums and moving belts. Moving belts are mainly applied in agriculture and rotating drums are mostly used for metals and plastics. (Higashiyama, Y. et al. 1998) This chapter concentrates on the rotating roll electrode which is the type used in the experimental part.

In Figure 4 is presented a schematic description of a roll-type electrostatic separator with one rotating roll electrode.

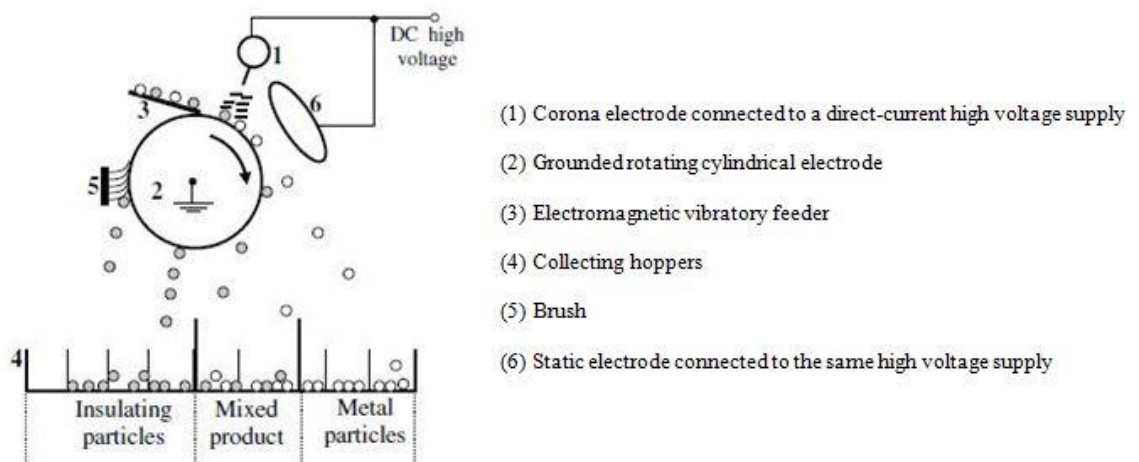


Figure 4 Schematic description of a roll-type electrostatic separator (Tilmaline, A. et al. 2009).

In general, the roll-type separator consists of a grounded rotating roll electrode and other active electrodes that are connected to a high voltage direct-current supply. The granular mixture to be separated is fed on the surface of the rotating roll at a certain speed and exposed to the electric field generated between the roll electrode and active electrodes. (Wu, J. et al. 2008) Separation devices making use of both corona and induction charging seem to be the most adequate ones. (Dascalescu, L. et al. 1998)

In Figure 5 are presented corona and induction charge models.

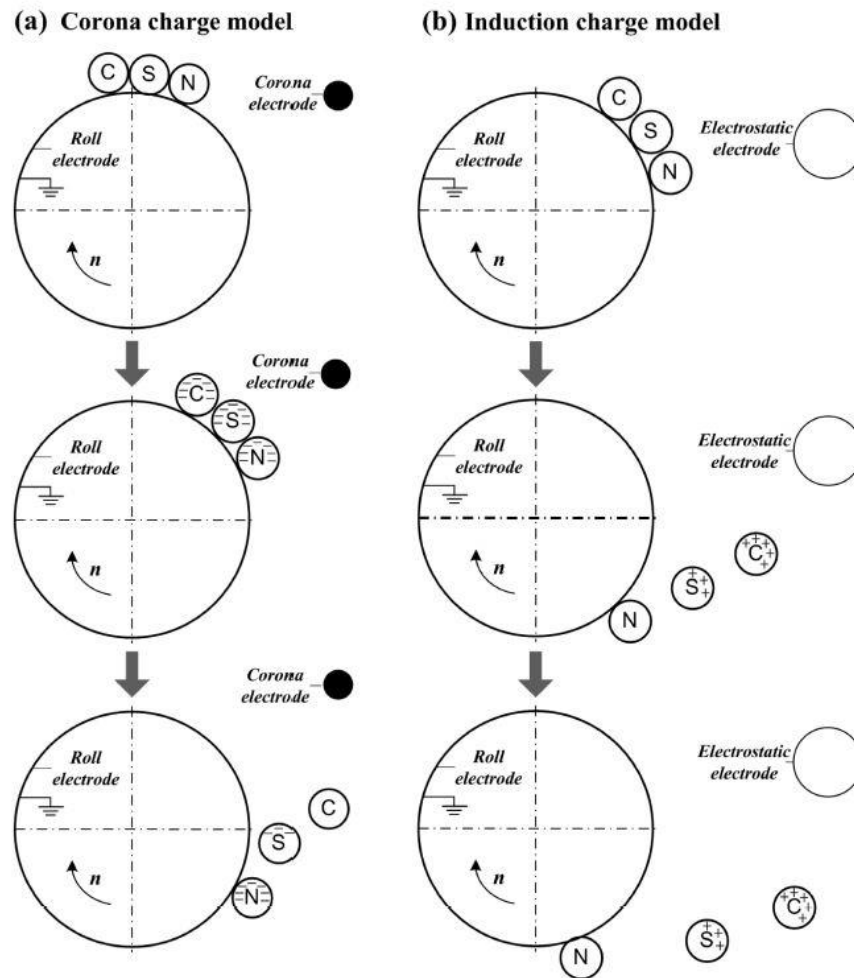


Figure 5 Charge model of conductor (C), semiconductor (S) and nonconductor (N) (Xue, M. et al. 2012)

In the corona charge model the corona electrode ionizes the air around it and causes electron current to flow to the grounded roll electrode. The particles that pass the ionized area are negatively charged by ion bombardment. Nonconductors keep their charge and adhere to the surface of the rotating roll, whereas conductors discharge rapidly to the roll electrode and detach from it. Semiconductors release partial negative charge and also detach from the roll, but slower than conductors. (Xue, M. et al. 2012)

After the ionized area the particles reach the electric field created by the electrostatic electrode. The electric field does not influence the non-conductive material, but charges the conductive particles which are then attracted towards the electrostatic electrode and collected in the right side of the collector (Dascalescu, L. et al. 1998). The insulating

particles pinned to the rotating roll fall down into the collector when the gravitational force becomes greater than the electric image force. In case some particles will not fall down, the separators usually have a brush that detaches mechanically the remaining particles from the surface of the roll. Also a “neutralization electrode” that eliminates the electric charge can be used to remove the particles from the surface. (Tilmaline, A. et al. 2009)

3.1.2 Parameters affecting to separation efficiency

The two notable problems affecting the efficiency and stability of the corona electrostatic separation process are particle aggregation and high voltage breakdown. By adjusting the parameters and operating conditions right the problems can be minimized and separation efficiency maximized. The parameters affecting most to the separation efficiency of corona electrostatic separator are electrode system, moisture content, rotor speed and particle size. (Cui, J. et al. 2003) Also materials of construction of the rotating roll, shape of the rotating roll, and temperature and pressure in the room the experiments are conducted in have an impact to the separation results. The parameters that can be affected to in the user phase are particle size, roll speed, moisture content of the material, operating parameters, and to some extent ambient conditions. By adjusting the dc high-voltage level, the feed rate and the roll speed the efficiency of the electrostatic separation can easily be controlled (Vlad, S. et al. 2000b)

Particle size

Particle size has a great impact to the separation results of corona electrostatic separator. With granular mixture containing coarse non-conducting particles the separators tend to throw non-conductors into the conductor collection due to their greater mass and momentum derived from the spinning roll. (TiTan Metallurgical Services. 2014) Very fine particles in turn may cause aggregation, which leads to poor separation results as well. (Li, J. et al. 2007)

Particle size ranging from 0.6 to 1.2 mm has been identified to be the most suitable for corona electrostatic separation in industrial applications by Li et al. (2007). They investigated the corona electrostatic separation of crushed waste printed circuit boards with five size classes of particles: (1) 0.8-1.2 mm, (2) 0.6-0.8 mm, (3) 0.45-0.6 mm, (4)

0.3-0.45 and (5) <0.3 mm. The results showed that production capacity and separated metal content were higher with size classes 1 and 2 than with the other size classes. The size class five was found to be unsuitable for electrostatic separation, because of the effect of aggregation. (Li, J. et al. 2007) However, Wu et al. present in their article (Wu, J. et al. 2009) that the optimum particle size for effective electrostatic separation of waste PCB is 0.1-0.6 mm, because the liberation between metals and non-metals will not be perfect with bigger particles. These differences in recommended particle sizes are probably due to different materials used, even though PCB was used in both studies. The prerequisite for successful separation process is the proper dissociation of different materials, and if that is not possible with slightly bigger particle sizes (for example 0.6-1.2 mm), the separation need to be carried out with smaller particle sizes.

Ultra-fine powders

Wu et al. analysed the impact of nonconductive powder (<0.045 mm) on electrostatic separation for recycling crushed waste printed circuit board. Ultra-fine particles have large specific areas and intensive surface free energies, which results in an intensive surface effect and aggregation. Some conductive particles may get enfolded by these aggregates, forming big non-conductive particles that adhere to the roll and fall to the middling collection. Obviously this weakens the separation results. Another problem with ultra-fine powders is the dust accumulation on the surface of corona electrode and electrostatic electrode. This happens with all granular mixtures, but fine powders increase the phenomenon significantly. Dust accumulation has negative influence to the distribution of electric field and space charges and leads to weakening of the electric field. Wu et al. found that when the nonconductive particle content was more than 10 %, it had strong negative influence to the separation. (Wu, J. et al. 2007)

Rotating roll speed

The speed of the rotating roll that spins around as the feed is fed into the machinery affects to the separation efficiency to some extent. Therefore it is advisable to conduct experiments with different roll speeds and measure the amount of middling collected to identify the optimum speed. The speed that produces the least amount of middling will be the most effective speed. In industrial scale when intention is to maximize the profit

it is appropriate to maximize the roll speed to gain greater output. In that case it should be taken into account that extremely high speeds can affect the purity and quality of the product. (Merahfe, K. 2011)

Li et al. have analyzed the affection of roll speed to the separation efficiency. They found out that the greater the rotational speed, the greater the recycle percentage of metal particles and the purity of nonmetal particles, but the worse the recycle percentage of nonmetal particles and purity of metal particles. (Li, J. et al. 2008) The reason is that when the roll speed increases, the metal particles detach easier from rotating roll electrode and thus end up more accurately to the metal collection bin, but at the same time the risk that also some nonmetal particles detach too early and end up to the same bin increases.

Li et al. suggests three ways to settle the problem: (1) increasing the electric field strength, width of corona field and the number of corona electrodes; (2) increasing applied voltage and decrease discharge gap and (3) changing the curvature of rotating roll electrode and position of corona electrodes. The first method increases the charging critical rotational speed, the second method is to avoid spark discharge and the third one decreases the loss of charge value on the surface of rotating roll electrode. Li et al. investigated that with the rotational speed of 70 rpm the purity and recycle percentage of materials got a good level. (Li, J. et al. 2008a)

Moisture content of the material

Dascalescu et al. have investigated the impacts of material moisture content to the separation efficiency in the case of PVC-metal electroseparation and found out it has a considerable influence on the separation results. The elevated moisture of the nonconductive grains causes them to depart from the rotating roll before touching the wiping brush. This increases the amount of middling, lowers the purity of metal collection and diminishes PVC recovery. Humid metal particles tend to adhere to the surface of the rotating roll, which decreases the purity of PVC and reduces metal recovery. With the moisture content of less than 0.3 % the technology was found to be efficient, so the feed material should be heated before separation to remove the moisture. (Dascalescu, L., et al. 1994)

Operating parameters

Constructions of electrodes, shapes and sizes of static electrodes, applied voltages, center distances and positions of electrodes affect to the electric field which affect to different trajectories of particles and thus separation efficiency. Li et al. have theoretically analyzed the influence of operating parameters to the distributions of electric field and separating results in the case of printed circuit boards, and used MATLAB to simulate the distribution of electric field in separating space. Through the correlation of simulated and experimental results, the optimum parameters for efficient separation were found to be the following: $U = 20\text{-}30\text{ kV}$. $L = L_1 = L_2 = 0,21\text{ m}$, $R_1 = 0,114$, $R_2 = 0,019\text{ m}$, $\theta_1 = 20^\circ$ and $\theta_2 = 60^\circ$. (Li, J. et al. 2008b)

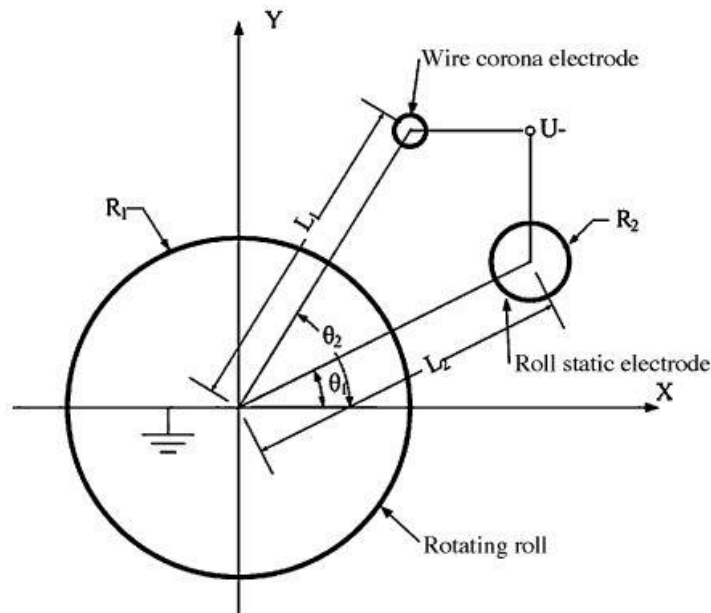


Figure 6 Operating parameters of corona electrostatic separator (Li, J. et al. 2008)

Ambient conditions

Temperature, pressure and humidity may have a great impact to separation results, especially if they vary significantly in a room or area where the process is run. Controlling these variations can be very difficult and costly, but experiments about the effects that variations have on separation results would give a good estimate about whether it would be a good investment to install controlling equipment or not. (Merahfe, K. 2011)

Shape of the rotating roll

Shape of the rotating roll determines the time the particles are exposed to the voltage in the electrostatic separation process. The larger the diameter of the roll, the larger the surface area and the longer the time the particles spend in the electric field. The shape of elongated cylinder enables longer time in the electric field than cylindrical or oval. By conducting experiments with different roll shapes would provide information about whether it would be advantageous to expose the particles to the voltage for a long or short amount of time. (Merahfe, K. 2011)

3.1.3 Applications

Corona electrostatic separation has applications ia. in minerals processing industry, in agriculture and in recycling. The separation in minerals processing relies on the different conductivities of ores: for example rutile (TiO_2) and iron pyrite (FeS_2) exhibit good conductivity, whereas quartz (SiO_2) and zircon (ZrSiO_4) exhibit poor conductivity. (Chang, J. et al. 1995) In the recent years the separation of electronic waste, especially printed circuit boards, with corona electrostatic separator has been under wide interest (Cui, J. et al. 2003), and at present it seems to be one of the most important applications of CES. The extreme difference in density and electrical conductivity of metallic and nonmetallic materials provides an excellent condition for the application of corona electrostatic separation in PCB recycling. (Cui, J. et al. 2003)

3.2 Plate-type electrostatic separation

The plate-type separator is used mainly for the sorting of fine granular material containing conducting particles, for example aluminium and copper particles. (Tilmaline, A. et al. 2009) Plate-type electrostatic separators utilize induction to separate the particles with different conductivities. (Higashiyama, Y. et al. 1998) The separator typically consists of a vibratory feeder, an inclined grounded metallic plate and a high-voltage static electrode. The plate that works as a passive electrode is usually S-shaped and in order to avoid edge effects the active high-voltage electrode has elliptical shape. (Vlad, S. et al. 2000a) In Figure 7 is presented a schematic description of a plate-type electrostatic separator.

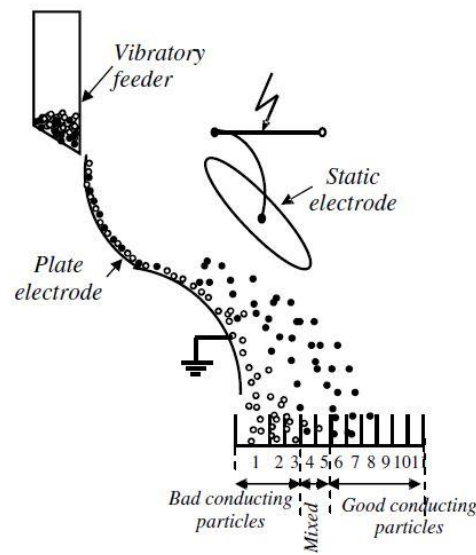


Figure 7 Schematic description of a plate-type electrostatic separator (Tilmaline, A. et al. 2009)

The granular material to be separated is fed to the surface of the grounded plate electrode by a vibratory feeder. Particles with poor conductivity are not attracted by the static electrode and thus slide down the plate and drop on the left side of the collector under the action of their mass and their speed. (Tilmaline, A. et al. 2009) Instead, granules with good conductivity charge by conductive induction in contact with the grounded plate. (Vlad, S. et al. 2000a) When the particles reach the zone of the electric field generated by the static electrode, they are subject to an attractive electric force exerted by this electrode and thus end up to the right side of the collector. (Tilmaline, A. et al. 2009)

The particular spot where a particle falls on the collecting plate is affected by its conductivity, mass density, dimension and shape and also by the strength of the electric field at the surface of the plate and by the voltage of the static electrode. (Vlad, S. 2001) Electrical and gravitational forces in plate-type electrostatic separation are smaller than those in corona electrostatic separation and the separation is generally less efficient overall, but the grain size in case of coarse granular mixture does not affect at the same rate as in corona separation. Thus electrostatic plates can successfully be used after the corona separation to counteract the effect of grain size. (TiTan Metallurgical Services. 2014)

3.3 Triboelectrostatic separation

Triboelectrostatic separation can be used for sorting of insulating particles only, such as PVC and PE granules (Tilmaline, A. et al. 2009). The separation is based on a tribocharging phenomenon, when two electrically non-conducting particles with different surface properties get charged when they contact each other. One of the particles becomes more positive or negative with respect to another one, and thus they will have different trajectories in electric field. (Mach, F. 2014) The mechanism of charge transfer between two granules in tribocharging is generally believed to be based on electron transfer, ion transfer and material transfer, from which the electron transfer is the most important one (Wu, G. et al. 2013).

According to charging mechanism, the devices utilizing tribocharging are classified to be “solid single phase” or “gas-solid two-phase”. The “solid single phase” means that the interactions exist only among solid particles during the charging process, whereas the “gas-solid two-phase” means that the interactions exist between gas and solid to charge the mixed solid particles. The devices classified to solid single phase contain rotating tube, rotary blades and vibrating devices, and the gas-solid two-phase devices contain fluidized bed, cyclone and propeller-type tribocharger. After the tribocharging of particles the granule mixture is fed into an electric field separator. There are three different separator types: free-fall separator, roll-type-separator and vertical electric separator. (Wu, G. et al. 2013) Free-fall electrostatic separator is the most widely used in triboelectrostatic separation process (Wu, G. et al. 2013), so it is used as an example in the next chapter to demonstrate the operation of triboelectrostatic separator.

Figure 8 presents a schematic description of a triboelectrostatic separation process with free-fall separator.

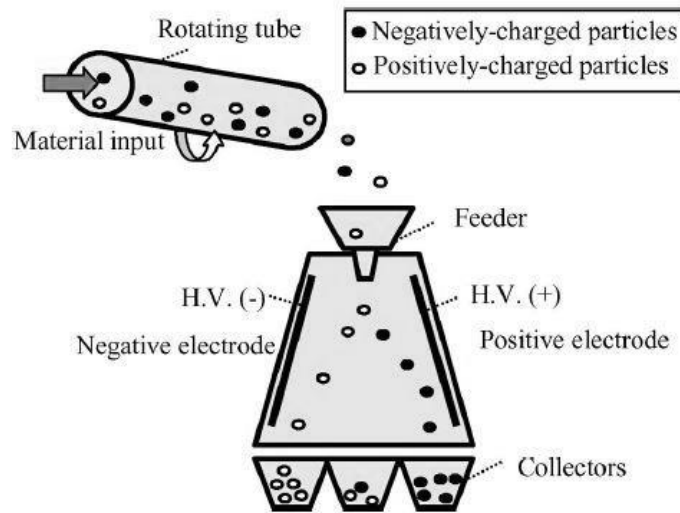


Figure 8 Schematic description of a triboelectrostatic separation process (Tilmaline, A. et al. 2010)

The particles to be separated get charged in a rotating aluminium cylinder by undergoing several collisions among themselves and against the cylinder wall. When particles exit the cylinder they fall vertically into a separator that consists of two metal electrodes of rectangular form. The electrodes are connected to two direct-current high voltage supplies and produce an intense horizontal electrical field between them. In the electrical field particles get different trajectories when particles negatively charged are attracted towards the positive electrode and the ones with positive charge are attracted towards the negative electrode. After falling through the electrical field, particles end up to different collection boxes according to their charge polarities. (Tilmaline, A. et al. 2009)

II Experimental part

Objective in experimental part is to carry out tests to investigate the effect of operating parameters on the separation results and find out if copper and precious metals in the test material could be enriched to the product. Chapter 4 presents the test equipment, concentrating on the corona electrostatic separator, and chapter 5 the analysing equipment of the samples. The compositions of the test materials, as well as the theoretical value of the materials are presented in chapter 6. In chapter 7 is presented the execution of the experiments and the experiments carried out including the parameter and variable values used in the experiments. Finally chapter 8 presents the results of the experiments, illustrating with figures the effect of the variables on separating results.

4 Test Equipment

4.1 Process and equipment

Figure 9 presents a photo of the test equipment.



Figure 9 Test equipment

The equipment consists of a feed hopper (Figure 10), vibratory feeder (Figure 11), multilevel vibrating screen (Figure 12), belt conveyor (Figure 13) and electrostatic separator (Figure 15).



Figure 10 Feed hopper



Figure 12 Screen



Figure 11 Vibratory feeder



Figure 13 Belt conveyor

Figure 14 presents a schematic description of the equipment and process.

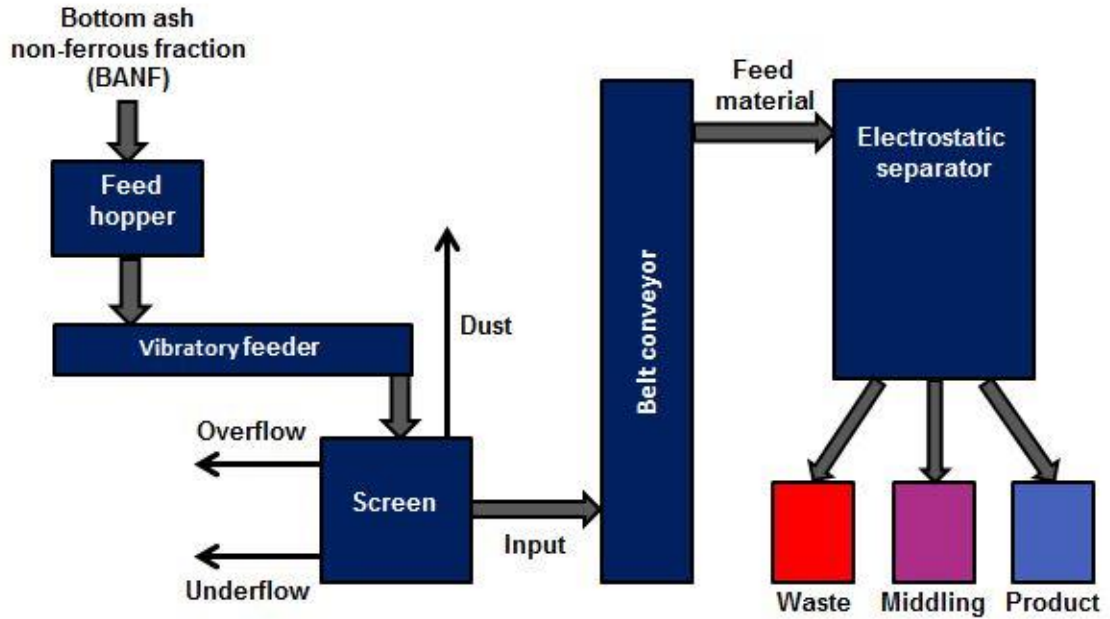


Figure 14 Schematic description of the equipment and process

The non-ferrous fraction of bottom ash, called BANF, is fed to the feed hopper, from which it flows to the vibratory feeder. The vibratory feeder feeds the material to the screen with speed that can be adjusted. The screen screens over 2 mm and under 0,28 mm particles to overflow and underflow, and the input material with size range of 0,28-2 mm is fed to the belt conveyor (additional experiment 4 is exception by its particle size range). The belt conveyor conveys the material with adjusted speed to the electrostatic separator which separates the feed material to three streams called product, middling and waste.

4.2 Electrostatic separator

Electrostatic separator used in this work is eForce[®] High Tension Electrostatic Separator for Minerals HT(36)121-50 by Outotec. Figure 15 presents a photo of the separator.



Figure 15 Electrostatic separator used in the experiments

The separator is a two-roll-type separator that utilizes both ion bombardment and static electrode to maximize the separation efficiency. It consists of two classical roll-type separation units arrayed in the vertical position. Both units have the same electrode configuration presented in Figure 16: a grounded roll electrode (1), a wire-type corona electrode (2) and a cylinder electrostatic electrode (3). After the upper separator a divider (4) divides the material to two streams.

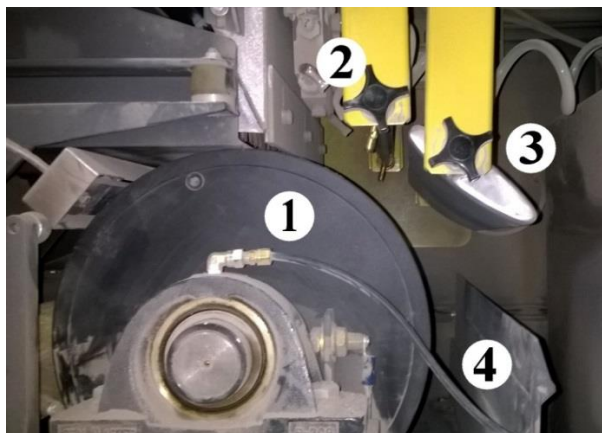


Figure 16 Configuration of the upper separation unit

The particles that are most affected by the static electrode end up to the right side of the divider and through a chute and pipe to the collection box on the right. The other particles fall to a hopper and are fed to the second separator, after which the particles are divided to three streams by two dividers. The most conductive ones end up to the right side of the right-hand divider to the same chute as part of the particles from the upper separator. The most insulating ones end up to the left side of the left-hand divider and through a pipe to the collection box on the left. The rest of the particles end up between the two dividers and through a pipe to the collection box in the middle.

In this work the fraction of particles that ends up to the box on the right and should contain the most conductive particles is called “**product**”, the fraction of particles that ends up in the middle is called “**middling**” and the fraction that ends up to the left and should contain insulating particles is called “**waste**”.

5 Analysing Equipment

The element contents of the samples were analysed with X-ray fluorescence (XRF) spectrometer and Inductively Coupled Plasma Optical Emission Spectrometer (ICP-OES). XRF was used to analyse copper contents of the samples, and ICP-OES the precious metal contents, because XRF could not recognise such a small contents as precious metal contents in the samples. Besides, ICP-OES analysis is more accurate and reliable than XRF. But because of the late installation of ICP-OES, only selected samples could be analysed with it. As pre-treatment for XRF analysis the samples were comminuted in disc mill. Composition and oxide layers of particles were briefly investigated with Scanning Electron Microscope (SEM).

5.1 X-Ray Fluorescence (XRF) spectrometry

The XRF spectrometer used in this work is Epsilon 3 XL by PANalytical, presented in Figure 17. It is a bench-top ED (energy dispersive) XRF spectrometer designed for elemental analysis in industry process control and research and development.



Figure 17 XRF spectrometer used for element analysis

The spectrometer consists of an X-ray tube, filters, sample changer, detector, pre-amplifier, amplifier and Multi Channel Analyzer (MCA). In the x-ray tube electrons from the filament strike the anode causing X-rays to be generated. Some of the X-rays pass through the window in the tube and may be filtered before irradiating the sample. The high energy electrons of the radiation penetrate the outer orbitals of the atoms in the sample and collide with electrons in the inner orbitals causing them to be ejected from the atom. To restore the stability, an electron from a higher energy level orbital will be

transferred to the lower energy level orbital. This transition releases energy as X-rays that are related to the atomic number of the atom producing them and are thus characteristic to a certain element. The characteristic x-rays are processed by the amplifiers and the MCA, after which the energy spectrum is produced. (PANanalytical. 2011)

5.1.1 Disc mill

The disc mill used to comminute the sample material homogenous enough for the XRF spectrometer is vibratory disc mill RS200 by Retsch, presented in Figure 18.



Figure 18 Disc mill used for grind the samples

The comminution is based on impact and friction. The grinding set is attached to the vibration plate with a quick-action lever, and the plate with the grinding set is subjected to circular horizontal vibrations. The grinding rings in the dish are affected by centrifugal force, which results in extreme pressure, impact and frictional forces acting on the sample, comminuting the particles. (Retsch. 2014)

5.2 Inductively Coupled Plasma Optical Emission Spectrometry (ICP-OES)

The model of the ICP-OES spectrometer used in the element analysis is Optima 8300 from PerkinElmer, presented in Figure 19.



Figure 19 ICP-OES used for element analysis

ICP-OES is one of the most important device in element analysis. It can be used to analyse even 70 elements' concentrations and the detection limits of different elements are low enough for most analysis. The method is based on extremely high temperature plasma that breaks the chemical bounds of compounds and thus produces atoms and ions. In plasma the atoms and ions excite, after which they emit the absorbed energy as fotons. The wave lengths of the emitted fotons are characteristic to certain elements, which makes it possible to recognize the elements. By utilizing the emissions intensities detected with certain wave lengths the concentrations of the elements can be determined. (Boss, B. and Fredeen, J. 2004)

5.3 Scanning Electron Microscope

The Scanning Electron Microscope (SEM) used in this work is LEO 1450, presented in Figure 20.

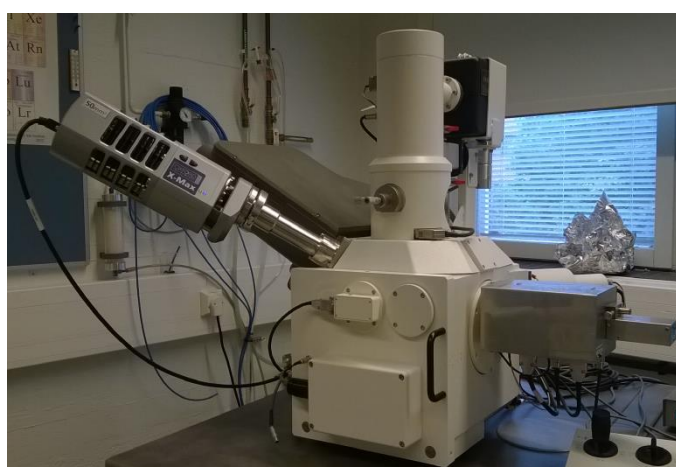


Figure 20 Scanning Electron Microscope used for analysis of the particle surfaces

SEM is commonly used to show spatial variations in chemical compositions and to generate high-resolution images of shapes of objects. SEM produces information by scanning the sample with focused beam of high-energy electrons. The electron-sample interactions generate a variety of signals that can be detected and that reveal information about the sample. In example secondary electrons and backscattered electrons are used for imaging samples, and characteristic X-rays are used for elemental analysis. (Integrating Research and Education. 2014)

6 Test Materials and Characterization

6.1 Material

Material used in the tests is fine (0-2 mm) non-ferrous fraction of the bottom ash from a Nord European plant. The plant is based on grate incineration technology and uses municipal solid waste and waste from industry and trade. The material used in the experiments has gone through magnetic separation, which removes ferrous material, and eddy current separation, which separates non-magnetic fraction. The non-magnetic fraction is then screened with 2 mm screen. Before screening, part of the fraction goes through rotor impact mill. **Thus, two fine non-ferrous bottom ash fractions are used in the tests:**

- Material called F12, which has gone through rotor impact mill

- Material called F5, which has not gone through the mill

Both materials are dried for the experiments, except for one experiment in which the effect of moisture content of the material was investigated.

6.1.1 Rotor impact mill

The rotor impact mill through which the material F12 has gone through is a vertical-shaft crusher equipped with impeller rotor and toothed anvil ring. It selectively crushes and separates composite materials, singles out entangled materials, reduces the size of brittle-hard materials and shapes metals into balls and cleans them. When the input material is fed into the machine, it hits the rotor and is accelerated outward by the centrifugal forces. The horseshoe-shaped hammers impel the material against the anvil ring which repels the material and makes it hit the hammer again. This process is repeated several times, resulting in selective and intensive stressing of the input material and ball-shaping of metals. The material leaves the rotor as soon as it is small enough to fit through the gap between the rotor and the anvil ring. (BHS. 2014)

6.2 Characterization

Materials F5 and F12 were characterized by screening the fractions to several size fractions, weighing the fractions and analyzing the fractions with XRF, ICP and SEM. The samples were taken from the input stream of the electrostatic separator (0,28-2 mm) and from the underflow (< 0,28 mm) and overflow (> 2 mm) of the screen.

To be able to combine the results of input and underflow sample analysis, the fractions of sieve underflow, input and overflow were determined by weighing the output fractions and underflow and overflow fractions after each experiment. The average values for F5 and F12 screen fractions are presented in Table 6. The variation in the fraction weighs between different experiments was approximately ± 2 %-points. As can be seen from the Table 6, the material F12 is much finer than F5, due to the treatment in rotor impact mill.

Table 6 F5 and F12 mass fractions of input, screen underflow and screen overflow

	F5	F12
underflow fraction (<0,28 mm)	11 %	41 %
input fraction (0,28-2 mm)	60 %	54 %
overflow fraction (>2 mm)	29 %	5 %

6.2.1 Sieving

The input and underflow samples were sieved with AS200 Analytical Sieve Shaker by Retsch, presented in Figure 21.



Figure 21 AS200 Analytical Sieve Shaker by Retsch

Input samples were sieved with 2 mm, 1 mm, 500 μm and 250 μm sieves and underflow samples with 250 μm , 125 μm , 63 μm and 45 μm sieves. After the sieving the fractions were weighed. The distribution of the particles to different size fractions in F5 and F12 are presented in Figure 22 below. The amount of screen overflow has also taken into account when calculating the mass fractions.

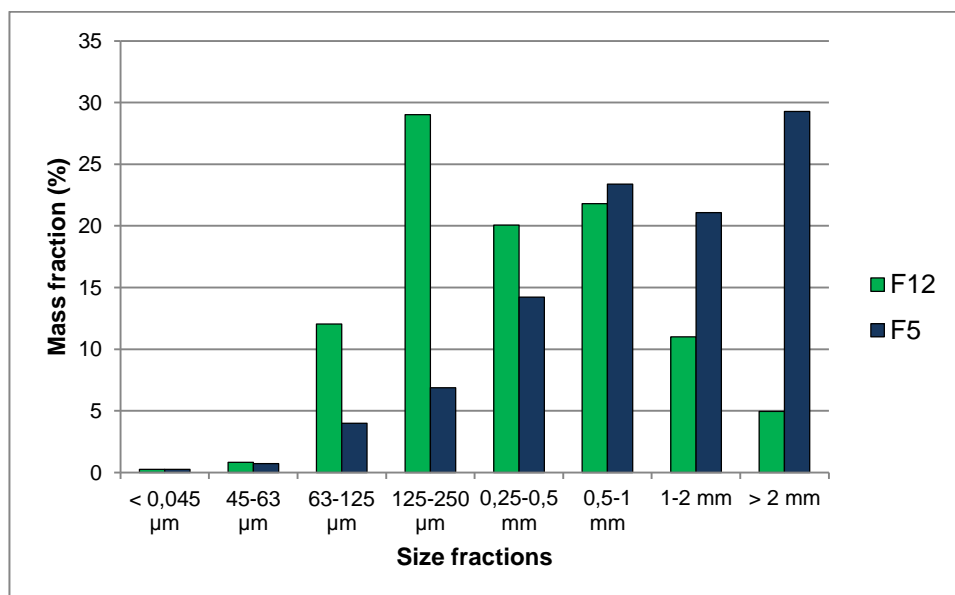


Figure 22 Mass distribution of particles to different size fractions in materials F5 and F12.

From Figure 22 can be seen that F5 is much coarser than F12. Approximately 70 w-% of the particles in F5 belong to the size range of $> 0,5$ mm by diameter, whereas the corresponding amount in F12 is approximately 38 w-%. Notable is that the biggest amount of particles in F5 belong to the > 2 mm size class, even though both materials have gone through 2 mm screen and theoretically should not contain > 2 mm particles. Notable is also that in F12 the biggest amount of particles is in the size class as fine as 125-250 μm , and the amount of particles under 63 μm is negligible in both materials. The latter is probably affected by the dust collection system to which the finest particles end up.

6.2.2 XRF and ICP analysis

The input sieve fractions of $> 2\text{mm}$, 1-2 mm, 500 μm - 1 mm and 250-500 μm , and underflow sieve fractions of 125-250 μm , 63-125 μm , 45-63 μm and <45 μm were analysed with XRF and ICP to investigate the distribution of elements, especially copper and precious metals, to different size fractions. The preliminary analysis of the copper and precious metal contents was made with XRF, and more accurate analysis later with ICP. According to the ICP results and sieving results presented in Figure 22, the amounts of copper and precious metals in different size fractions of the materials were calculated. The results are presented in grams of metal per ton of BANF.

Below are presented the analysis results for both materials.

Material F5

Figure 23 shows that the content of silver in F5 is significantly higher than the contents of other precious metals, especially in size fraction 45-63 μm . Gold has the second highest contents, and seems to concentrate slightly to three of the coarsest size fractions. Contents of palladium and platinum are almost non-existent, excluding size fraction > 2 mm which has a bit higher contents than the finer fractions.

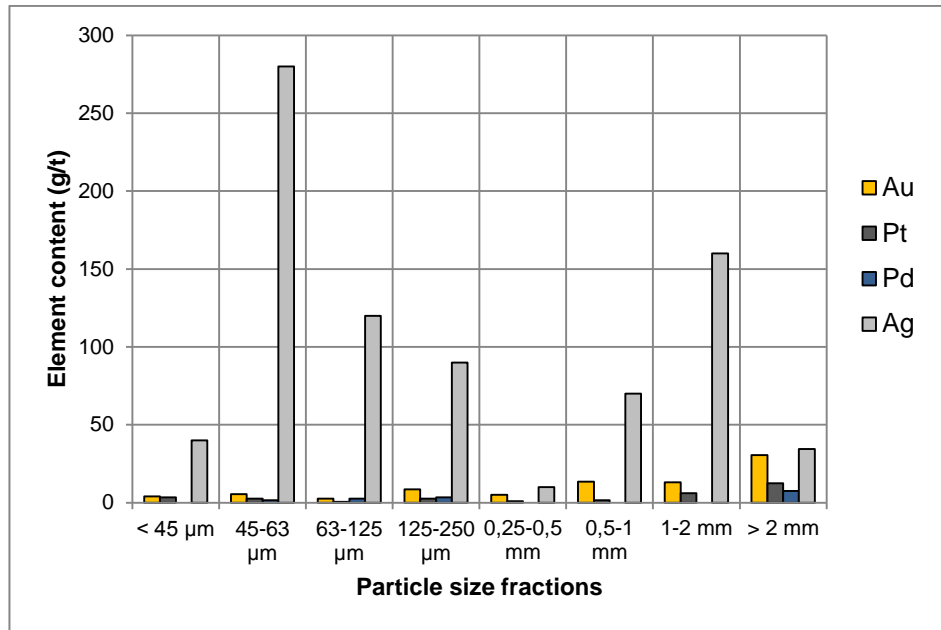


Figure 23 Material F5, precious metal contents in different size fractions based on ICP-analysis

Figure 24 presents the actual amount of precious metals in each size fraction in one ton of F5 BANF. As can be seen, despite the high silver content of 45-63 μm size fraction, the amount of silver that belongs to that size class in one ton of material is very small because the material consist mostly of coarser particles. The biggest amounts of silver can be found from size classes 0,5-2 mm, and biggest amounts of gold from size classes > 125 μm. Platinum and palladium appear in small amounts in size class > 2 mm.

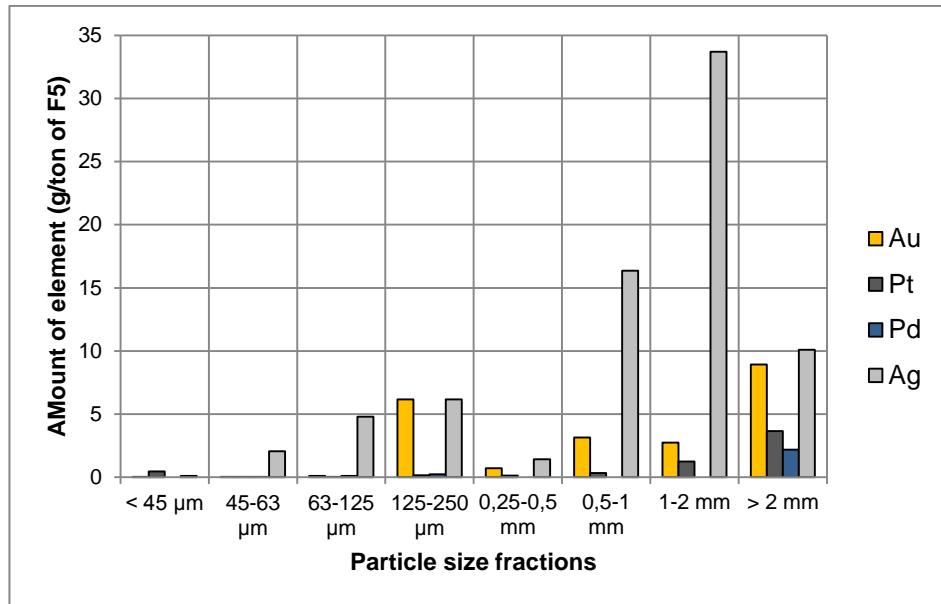


Figure 24 Material F5, amounts of precious metals in different size fractions per ton of F5. Results are based on ICP-analysis and mass distribution of particles to different size fractions (Figure 22)

Figure 25 presents the distribution of copper to different size fractions. As can be seen, the content is highest in the coarsest fraction, and that fraction also contains more copper than the other size fractions together: approximately 60 % of all the copper in the material belongs to the size fraction > 2 mm.

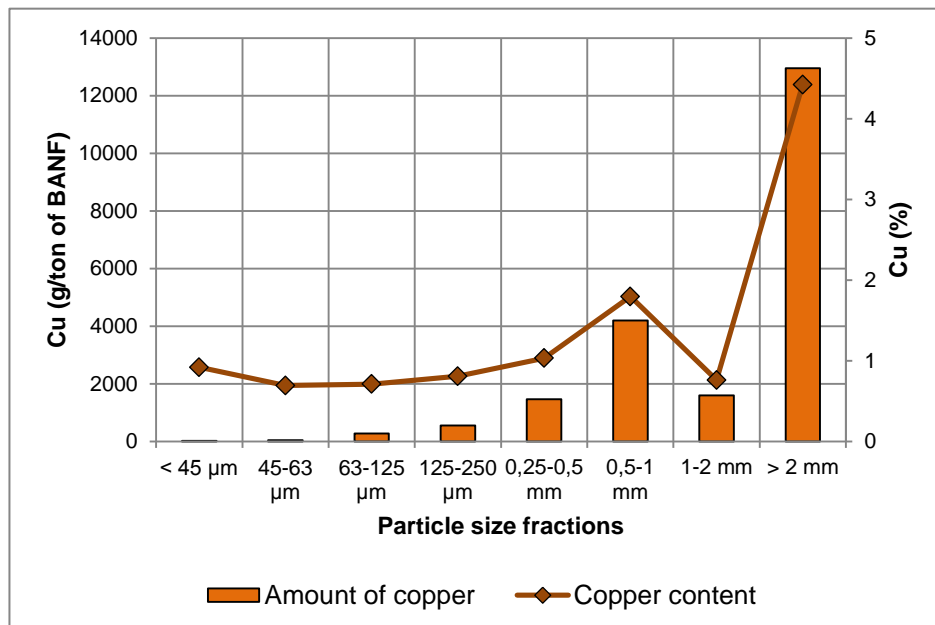


Figure 25 Material F5, copper contents and amounts of copper per ton of BANF. Results are based on ICP-analysis and mass distribution of particles to different size fractions (Figure 22).

Material F12

From Figure 26 can be seen that in material F12 silver clearly concentrates to the size fractions <63 μm . Content of gold is highest in the size fractions of <45 μm and 1-2 mm, and content of platinum in size fractions >1 mm. Palladium content does not have that much variation between different size classes, apart from size class <45 μm in which the content is zero. Figure 27 shows that even when the contents of precious metals seem to be the lowest in the middle size classes, the biggest amount of precious metals can be found from size classes 125-150 μm and 1-2 mm, in which especially the amount of silver is significantly higher than in other size classes.

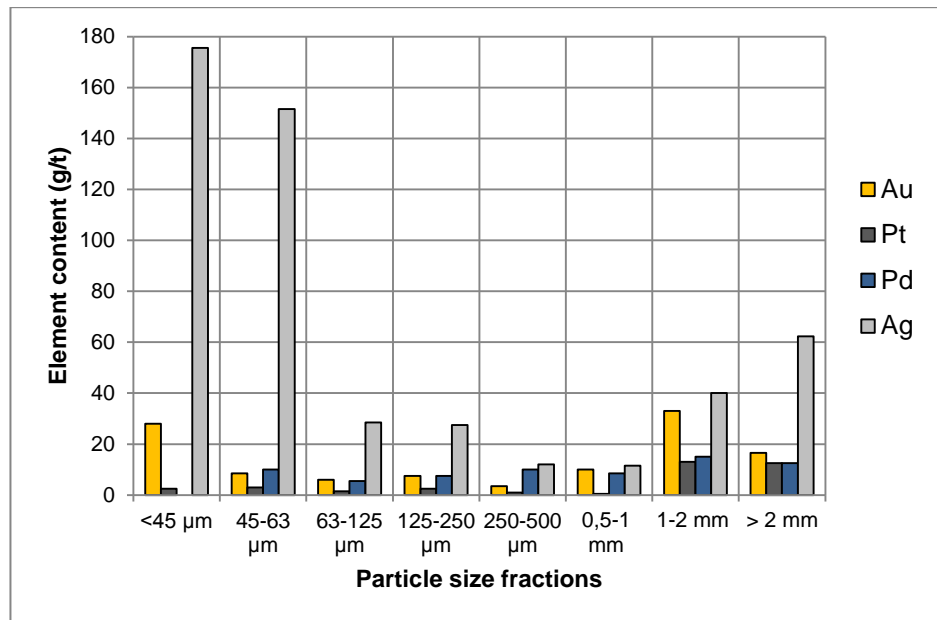


Figure 26 Material F12, precious metal contents in different size fractions based on ICP-analysis

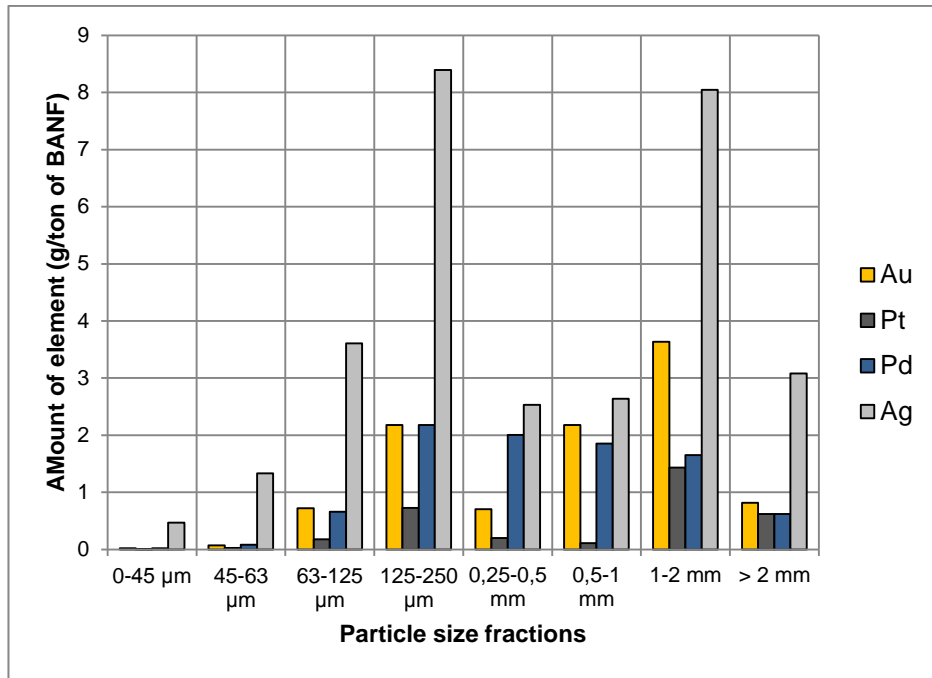


Figure 27 Material F12, amounts of precious metals in different size fractions per ton of BANF. Results are based on ICP-analysis and mass distribution of particles to different size fractions (Figure 22)

The same kind of phenomenon can be seen in Figure 28 which presents the copper content and amount in different size classes. The content is highest in the outermost size classes, but approximately 97 % of the feed material's copper is in the size classes > 63 µm.

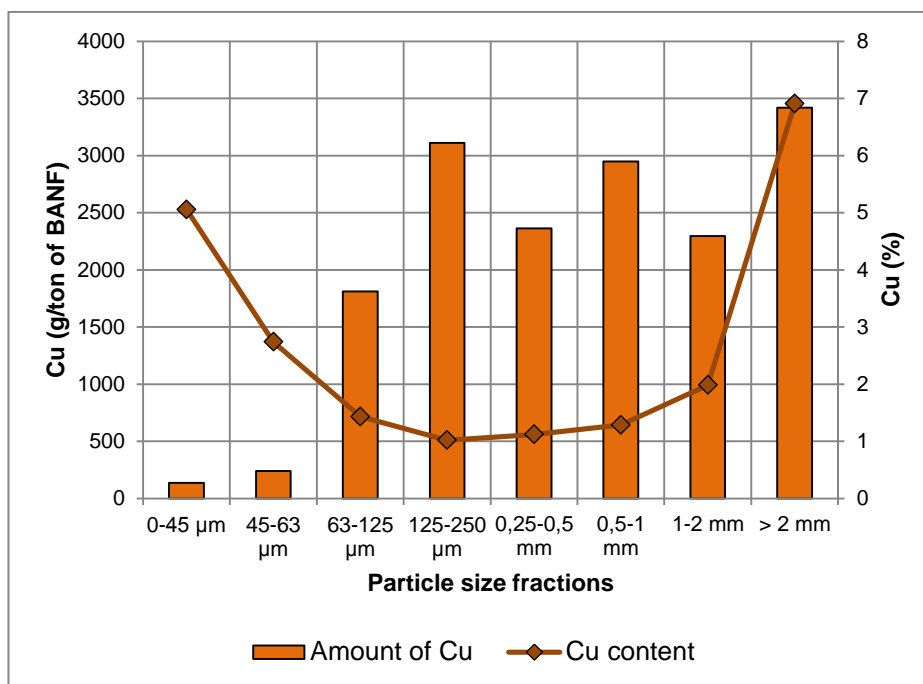


Figure 28 Material F12, copper contents and amounts of copper per ton of BANF in different size fractions. Results are based on ICP-analysis and mass distribution of particles to different size fractions.

When comparing the results of materials F5 and F12, can the effect of rotor impact mill be clearly seen. Especially Figure 24 and Figure 27 illustrate well how the mass of precious metals and copper concentrates in F5 to the coarsest fraction, but is in F12 more equally distributed. The difference between the total amounts of copper and precious metals in the materials is presented in chapter 6.3, in which the theoretical value for both materials is calculated.

6.2.3 SEM analysis

Scanning electron microscope (SEM) was used to analyze the cross section surfaces of the input particles. The purpose of the analysis was to investigate whether the particles have oxide layers on their surfaces which could hinder the separation, and if there is any difference in the surfaces of F5 and F12 particles. Samples were taken from both materials' input streams and sieved to size fractions of 1-2 mm, 0,5-1 mm and <0,5 mm.

For the SEM analysis small amount of particles from each sample were pressed to small carbon buttons which were then polished from the analysis surface. The analyses with the microscope were carried out by searching metal particles from the samples, zooming to the edge of the particle and taking element analysis from different phases. Pictures

were taken of the zoomed area and the whole particle, and thickness of the possible oxide layer was measured.

Because the sample preparation and SEM analysis were very time depending, and the samples contained relatively small amount of metal particles, the total amount of metal particles investigated was only 40; 5 particles from size fractions of <0,5 mm and 1-2 mm, and 10 particles from size classes of 0,5-1 mm. However, some information was still got about the particles' surfaces.

Results

From the results of the SEM analysis could be seen that every investigated metal particle had some kind of an oxide layer on its surface. In most of the cases the oxide layer consisted of aluminum oxide and/or calcium oxide, and was 10-30 μm thick. Any difference between the oxide layers of F5 and F12 particles could not be detected with this amount of investigated particles. Pure particles that would have included only one element was detected none; most of the particles were formed of several different phases. More research would be required to be able to say anything sure about the overall particle structure of the materials.

Below are presented few examples of investigated particles.

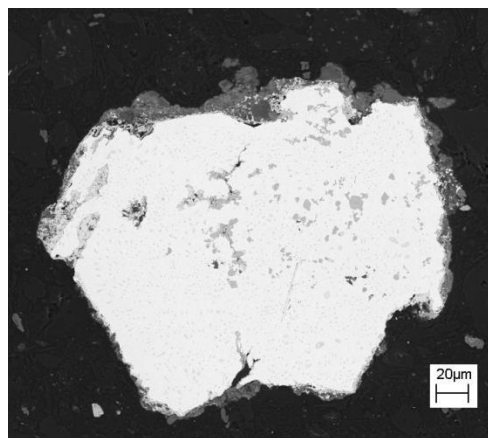


Figure 29 F5. Copper particle, with approximately 4-20 μm thick aluminium oxide layer on surface

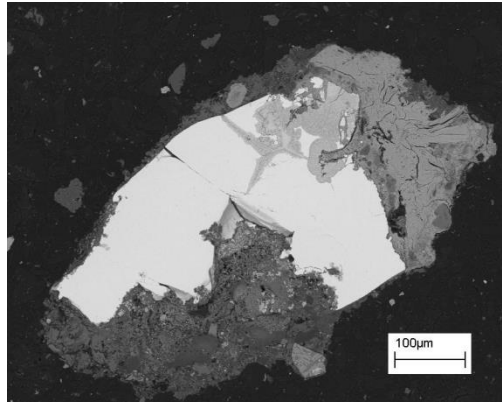


Figure 30 F5. Brass particle, surrounded by at least zinc oxide and copper oxide



Figure 31 F5. Particle with lead and oxides (aluminium, calcium, silicon). 10-20 μm thick oxide layer on surface

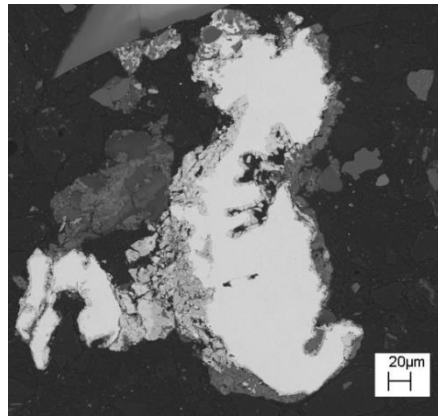


Figure 32 F12. Copper particle, with approximately 20 μm thick oxide layer consisting of copper and calcium oxide

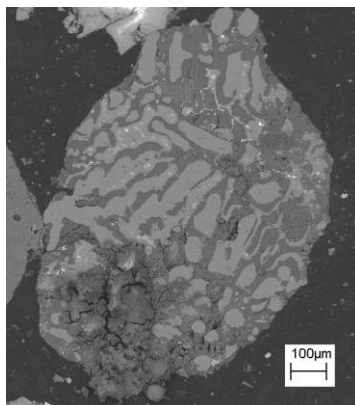


Figure 33 F12. Aluminium particle, with aluminium oxide and small spots of lead

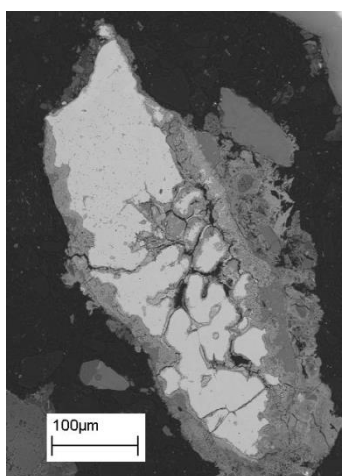


Figure 34 F12. Ferrite particle with nickel and chrome. Approximately 30-80 um thick oxide layer consisting of chrome oxide, calcium oxide and silicon oxide

6.3 Theoretical value

Theoretical value was calculated for BANF of F5 and F12 according to the ICP-analysis results of sieve fractions' copper and precious metals contents. The purpose of calculating the theoretical value is to show the value of copper and precious metals in one ton of BANF, and illustrate where the value of the materials comes from. However, **it has to be considered that the value is only theoretical and does not correspond by any means to the actual commercial value of the material.**

The values of the elements used in the calculations are from London Metal Exchange the average values of May 2014. Table 7 presents the values of the metals in London Metal Exchange, the contents of the metals in both materials and the values for one ton of the material.

Table 7 Total precious metal contents and values of the materials

Value/kg (€)		Material F12		Material F5	
		Content (g/t)	Element value in ton of material (€)	Content (g/t)	Element value in ton of the material (€)
Ag	482,6	30,1	14,5	74,8	36,1
Au	31294,8	10,3	323,1	21,9	684,6
Pd	20924,4	9,1	189,8	2,5	53,3
Pt	35127,8	3,3	115,8	6,1	214,0
Rh	32985,7	0,6	20,0	0,0	0,0
Cu	5,2	16326,4	85,3	21147,3	110,4
		Total value/ton (€)	748,5	Total value/ton (€)	1098,5

As can be seen, the calculated value of material F5 is much higher than the value of F12; mainly because of its higher gold content, but also the contents of silver, platinum and copper are higher in F5. It is possible that the difference is caused by rotor impact mill, if part of the precious metals is lost to the dust in the mill. It also have to be taken into account that the analysis results are only based on very small amount of material, which may cause that the results do not fully represent the reality.

Figure 35 and Figure 36 present how the values of the materials are distributed between different metals.

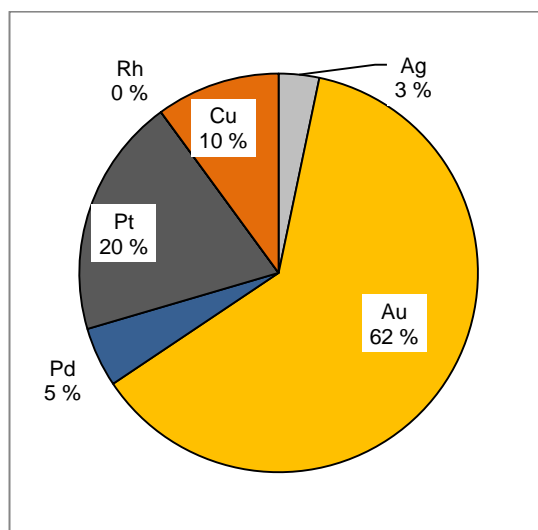


Figure 35 Formation of value in material F5

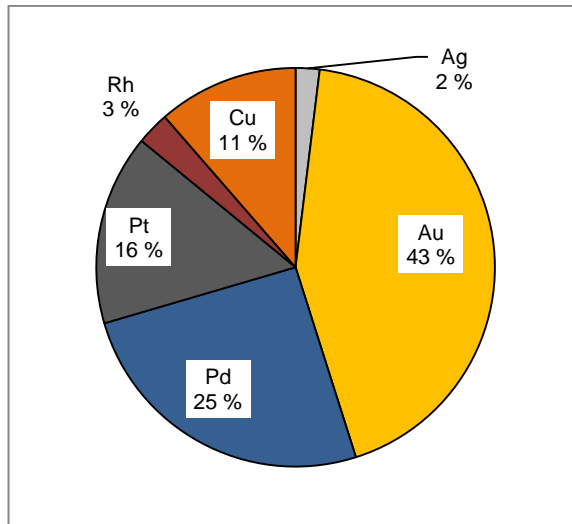


Figure 36 Formation of value in material F12

As can be seen, gold forms the biggest part of both materials' values. In F12 palladium has the second biggest fraction, but in F5 the fraction of palladium is only 5 %. Even though silver content is the highest of the precious metal contents in both materials, its price is so much lower than the prices of other precious metals that it forms only a couple of percent of the values. Copper also forms only a small part of the values despite its high contents in the materials.

7 Execution of Experiments

Each experiment was carried out in the same way. The equipment was turned on, parameters were adjusted and the separator was let to run few minutes. To investigate the mass fractions of different output streams, buckets were set under the streams for five minutes and then removed aside to wait for mass fraction measurements.



Figure 37 Sampling for determination of mass fractions



Figure 38 Samples waiting for weighing

In the case of reject, the amount of collected material was so small that it was suitable to be put to a sample bag and used in analysis. In the case of intermediate and conductor material, the amount of collected material was too big for this, so representative samples suitable for analysis were taken separately by holding a bucket under both streams for required time (approximately 20-25 seconds) to collect appropriate amount of material.



Figure 39 Sampling for element analysis



Figure 40 Sample for element analysis

After the sampling, the value of the parameter investigated in the experiment was changed, and the test was repeated. If needed, the equipment was turned off for the time of parameter adjustment. During each experiment samples were also taken from the screen overflow and underflow by holding a bucket under the stream appropriate time. From the input stream the sample was taken with a sand shovel from a hole made to a tube through which the input material flows from the screen to the conveyor belt.



Figure 41 Sampling from screen underflow



Figure 42 Sampling from feed stream

After carrying out the test with five different values of the investigated variable, the buckets and sample bags were weighed and photo of each sample was taken. Also the amounts of collected screen overflow and underflow matter were weighed, as well as the collection boxes of output materials.

7.1 Preliminary experiments

The purpose of pre-experiments was to find out how the equipment operates and how the different operating parameters affect to the separation. Five experiments were carried out, each of them testing the effect of one of the following operating parameters: voltage, roll speed, distance of corona electrodes, distance of static electrodes and distance of dividers. Distances of the parameters were measured perpendicularly from the rotating roll, and they were adjusted to be the same in both separation units. In each experiment the tested variable was given five values while the other parameters were

kept the same. Variable values in each test are presented in Table 8 and parameter values in Table 9.

Table 8 Variable values used in pre-experiments

PE nro	Variable	Values				
		Test 1	Test 2	Test 3	Test 4	Test 5
1	Voltage (kV)	20	22	24	26	28
2	Roll speed (r/min)	20	35	50	65	80
3	Distance of corona electrodes (mm)	40	45	50	55	60
4	Distance of static electrodes (mm)	50	55	60	65	70
5	Distance of dividers (mm)	70	80	90	100	110

Table 9 Parameter values used in pre-experiments

Parameter	Value
Voltage (kV)	26 (22 in experiment 3)
Distance of corona electrodes (mm)	55
Distance of static electrodes (mm)	65
Distance of dividers (mm)	100
Roll speed (rpm)	50
Feed rate	7
Conveyor line speed	10
Material	F5
Particle size range	0,28-2 mm

The voltage for the pre-experiment 3 was defined by searching the maximum value of voltage for the shortest distance of the electrodes (35 mm) with which the separator could be run without breakdown.

7.2 Main experiments

The objective of main experiments was to search for optimum values for run parameters using the results of pre-experiments, and investigate the effect of different combinations of variable values on the separation. In addition purpose was to investigate whether the processing with rotor impact mill affects to the separation by comparing the separation results of F5 and F12 materials with each other.

When planning the main experiments, only two samples of tests 1 and 5 from each pre-experiment were analysed with XRF, because the relatively late installation of the machine. Thus, the variable and parameter values for main experiments were chosen according to the XRF results of the few analysed tests of pre-experiments, and

according to the results of the determination of particle mass distribution to product, middling and waste. The main experiments are described below.

Main experiment 1 - Variable: Voltage

The results of the tests 1 and 5 in pre-experiment 1 (Figure 43 and Figure 44) indicated that the lower the voltage, the higher the copper content of product. But even with the lowest value of voltage in pre-experiment 1, which was 20 kV in the test 1, the copper content of product was only approximately 1,5 %. The objective of main experiment 1 was to test the sensitivity and selectivity of the electrostatic separator by creating weak electric field. The pre-assumption was that weak electric field could improve the selectivity of the separator and thus raise the copper content of product and improve product quality. To test this, the electrodes were adjusted as far as possible from the roll and test runs were carried out with voltages 14, 16, 18, 20, 22 and 24 kV. The values of run parameters are presented in Table 10.

Table 10 Values of parameters in main experiment 1

Parameter	Value
Material	F5
Particle size (mm)	0,28-2
Distance of corona electrodes (mm)	65
Distance of static electrodes (mm)	65
Distance of dividers (mm)	100
Roll speed (rpm)	50
Feed rate	7
Conveyor line speed	10

Main experiment 2 - Variable: Distance of corona electrodes

The results of pre-experiment 3 (Figure 47 and Figure 48) indicated that the distance of corona electrodes does not really have an effect on the copper content of product. However, in main experiment 1 lot of impurities ended up to the product with low voltages (Figure 56). The objective of main experiment 2 was to test if the distance of corona electrodes affects to the purity of the product with low voltage. Test runs were carried out with the corona electrode distances of 35, 45, 55, and 65 mm. Parameter values are presented in Table 11.

Table 11 Values of parameters in main experiment 2

Parameter	Value
Material	F5
Particle size (mm)	0,28-2
Voltage (kV)	16
Distance of static electrodes (mm)	65
Distance of dividers (mm)	100
Roll speed (rpm)	50
Feed rate	7
Conveyor line speed	10

Main experiments 3 and 4 - Variables: Voltage, distance of dividers, distance of corona electrodes

The objective of main experiments 3 and 4 was to investigate the effect of different combinations of chosen variables to the separation with both materials, and compare the results to investigate the effect of rotor impact mill. Each variable was given higher and lower values, and the test runs were carried out with all the combinations of the variables. Experiment 3 was carried out with material F5 and experiment 4 with material F12. In both experiments the same variable values were used to enable comparison between separation results of the two materials and evaluate the effect of rotor impact mill to the separation. The values of variables are presented in Table 12 and the values of parameters in

Table 13.

Table 12 Variable values in main experiments 3 and 4

Test nro	Voltage (kV)	Distance of dividers	Distance of corona electrodes
1	22	11	60
2	22	11	50
3	22	7	60
4	22	7	50
5	16	11	60
6	16	11	50
7	16	7	60
8	16	7	50

Table 13 Parameter values in main experiments 3 and 4

Parameter	Value
Material	F5 in experiment 3 F12 in experiment 4
Particle size (mm)	0,28-2
Distance of static electrodes (mm)	65
Roll speed (rpm)	50
Feed rate	7
Conveyor line speed	10

7.3 Additional experiments

The objective of additional experiments was to investigate the effect of few individual parameters to the separation. The parameters investigated were feed rate, distance of the upper roll's divider, moisture content of the material and dust in the feed material.

The effect of feed rate and distance of the upper roll's divider, investigated in additional experiments 1 and 2, were tested in the same way as the effect of variables in pre-experiments: by running tests with different variable values and comparing the test results with each other. In additional experiment 1, in which the effect of feed rate was investigated, the objective was also to calculate the capacity of the equipment.

The effects of moisture content and dust in the material were investigated in additional experiments 3 and 4 by running three tests with parameter values chosen from the tests made earlier with the same material, and comparing the results with the results of earlier tests. The values of the parameters and variables were chosen to be the same as in the tests 4, 5 and 8 in factor experiment made with material F12. Additional experiment 3 was carried out with un-dried F12, but the material was from different plant than the material in factor experiment, so the results cannot fully be compared with each other. Additional experiment 4 was carried out with dried F12, but the 0,28 mm screen was removed to let the dust enter the separator as well.

Table 14 presents the parameter and variable values of additional experiments 1 and 2, and Table 15 the parameter and variable values of additional experiments 3 and 4.

Table 14 Parameter and variable values in additional experiments 1 and 2

	Additional experiment 1	Additional experiment 2
Variable	Feed rate	Distance of upper divider
Material	F5	F5
Particle size (mm)	0,28-2	0,28-2
Voltage (kV)	16	16
Distance of corona electrodes (mm)	35	35
Distance of static electrodes (mm)	65	65
Distance of dividers (mm)	100	lower: 100 higher: 60, 80, 100, 120, 140, 160, 180
Roll speed (rpm)	50	50
Feed rate	5, 6, 7, 8, 9	8
Conveyor line speed	10	10

Table 15 Parameter and variable values in additional experiments 3 and 4

	Additional experiment 3	Additional experiment 4	
Material	Moist F12	Dry F12	
Particle size	0,28-2 mm	0-2 mm	
	Test 1	Test 2	Test 3
Voltage (kV)	22	16	16
Distance of corona electrodes (mm)	50	60	50
Distance of static electrodes (mm)	65	65	65
Distance of dividers (mm)	7	11	7
Roll speed (rpm)	50	50	50
Feed rate	7	7	7
Conveyor line speed	10	10	10

8 Results

8.1 Preliminary Experiments

In preliminary experiments the effect of chosen parameters on the separation was evaluated through the distribution of output material into product, middling and waste fractions and through the copper content of product. The copper amount per feed ton was also calculated to give an understanding about the copper amount that is actually recovered with chosen parameter values. Feed material means the material that is fed to the separator after the screen. In other words, the amount of recovered copper describes the relationship between copper content in product and product mass fraction. The purpose in pre-experiments was to investigate how much and in what way the change in each parameter's value affects to the separation results. Precious metal contents were not considered because there was not enough time to analyse the pre-experiment samples with ICP-OES.

8.1.1 Effect of Voltage

Results of pre-experiment 1 are presented in Figure 43 and Figure 44. Figure 43 presents the effect of voltage on output mass fractions and Figure 44 the effect of voltage on product's copper content and the amount of recovered copper.

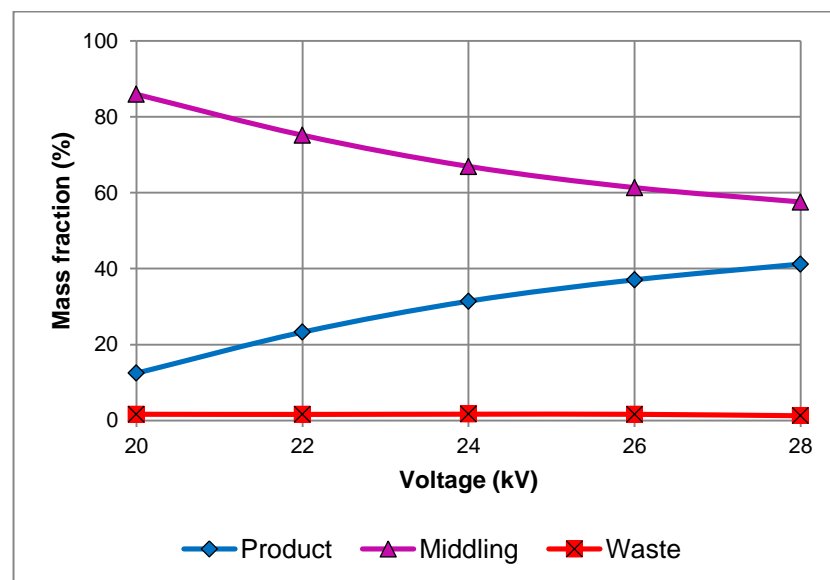


Figure 43 Effect of voltage on output mass fractions

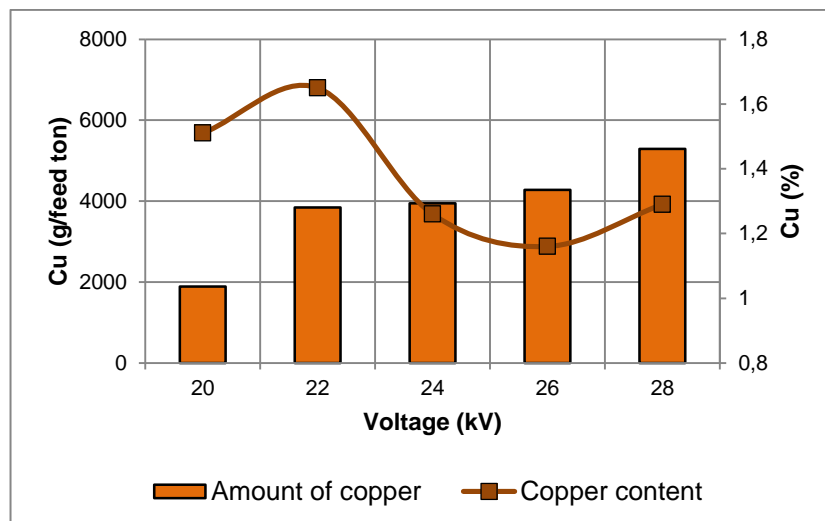


Figure 44 Effect of voltage on content and recovered amount of Cu in product

The results show that voltage has a significant effect on output mass fractions and product's copper content. Figure 43 illustrates how the mass fraction of product increases and the mass fraction of middling decreases when voltage is increased. Instead, the mass fraction of waste stays almost non-existent despite the changes in voltage. Figure 44 shows that the copper content is slightly higher with the lower values of voltage, but then the mass fraction of product is so small that the amount of copper ending up to the product with the lowest voltage is approximately 3400 grams less per ton of feed material than with the highest voltage.

8.1.2 Effect of roll speed

Figure 45 presents the effect of roll speed on output mass fractions and Figure 46 the effect of roll speed on Cu content in product and amount of recovered Cu.

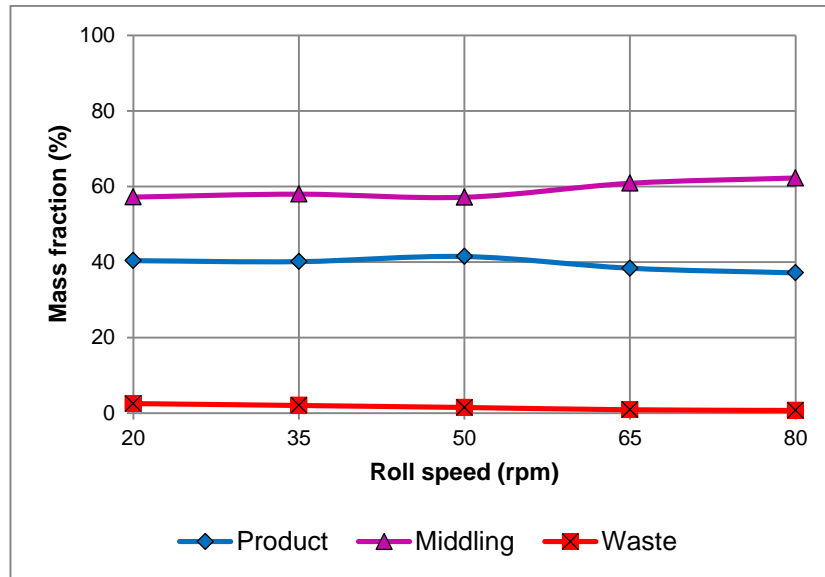


Figure 45 Effect of roll speed on output mass fractions

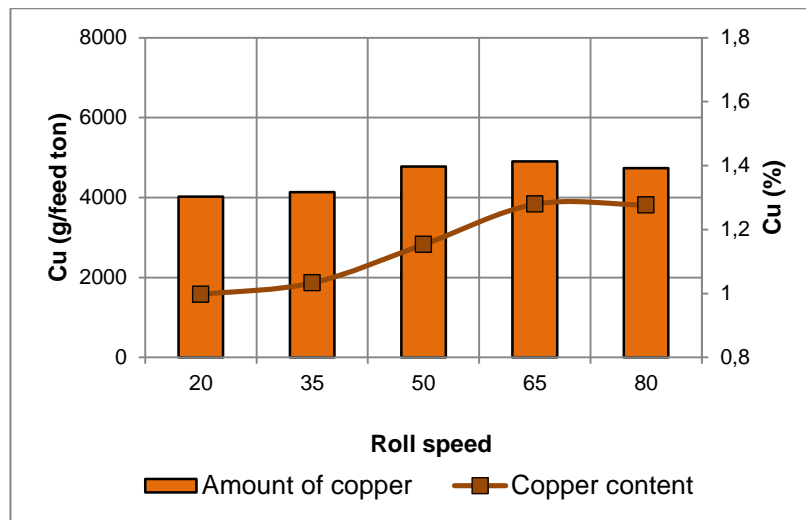


Figure 46 Effect of roll speed on content and recovered amount of Cu in product

The results show that roll speed barely affects to the particles' distribution into different fractions. Instead, roll speed has a minor effect on the copper content of product and thus also on the recovered amount of copper, as can be seen from Figure 46. With the roll speeds of 50-80 rpm the copper content is a bit higher than with the lower speeds, as well as the amount of recovered copper.

8.1.3 Effect of corona electrode distance

The effect of distance of corona electrodes on the output mass fractions is presented in Figure 47, and the effect of corona electrode distance on the copper content in product and recovered amount of copper in Figure 48.

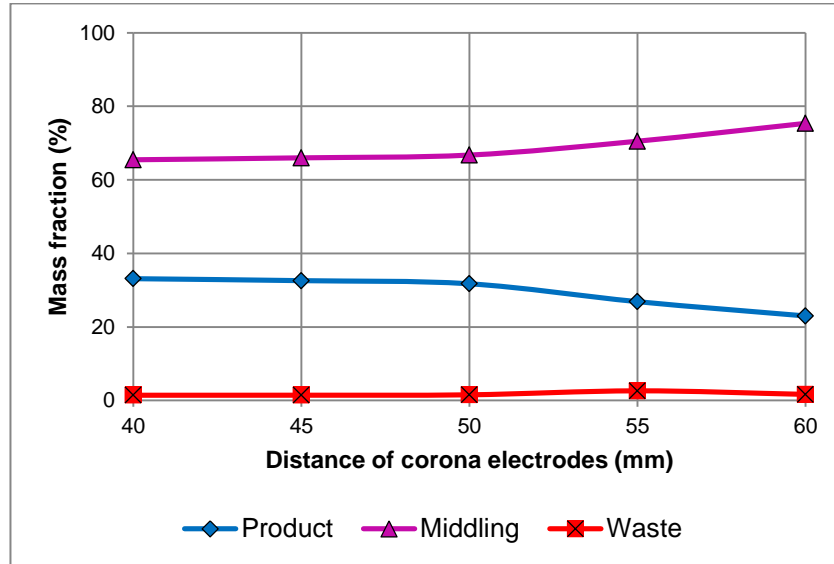


Figure 47 Effect of corona electrode distance on output mass fractions

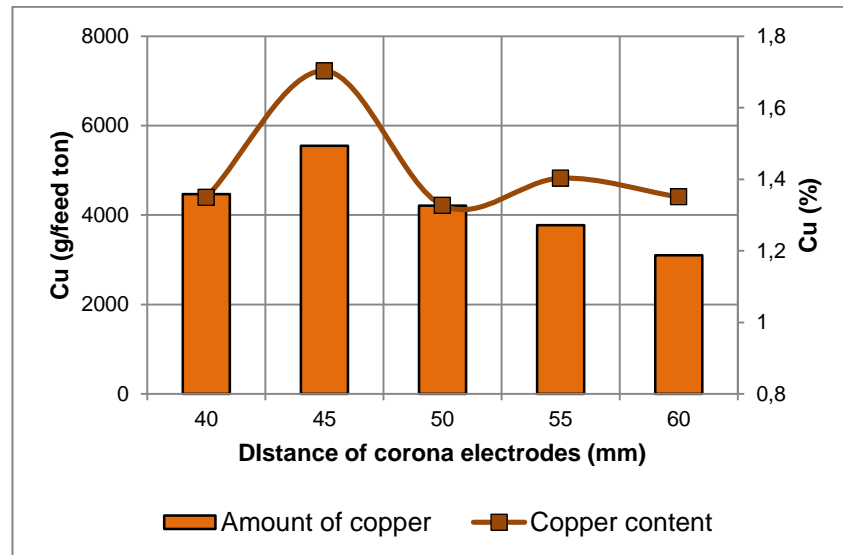


Figure 48 Effect of corona electrode distance on Cu content and amount in product

As can be seen from Figure 47, the distance of corona electrodes affects only a little to the mass fractions of product, middling and waste. Figure 48 shows that also the content and recovered amount of copper in product stay almost the same; only with the distance of 45 mm the content is slightly higher.

8.1.4 Effect of static electrode distance

The effect of static electrode distance on the output mass fractions and Cu content and amount in product are presented in Figure 49 and Figure 50.

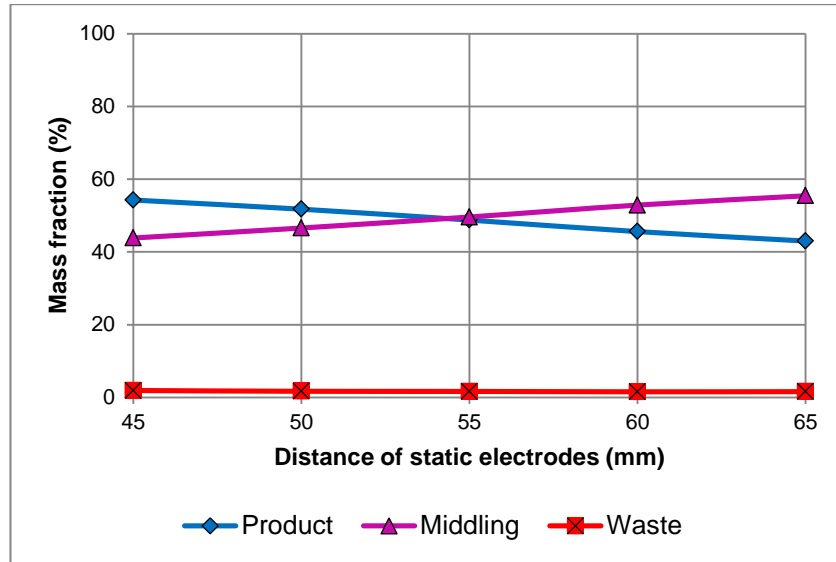


Figure 49 Effect of static electrode distance on output mass fractions

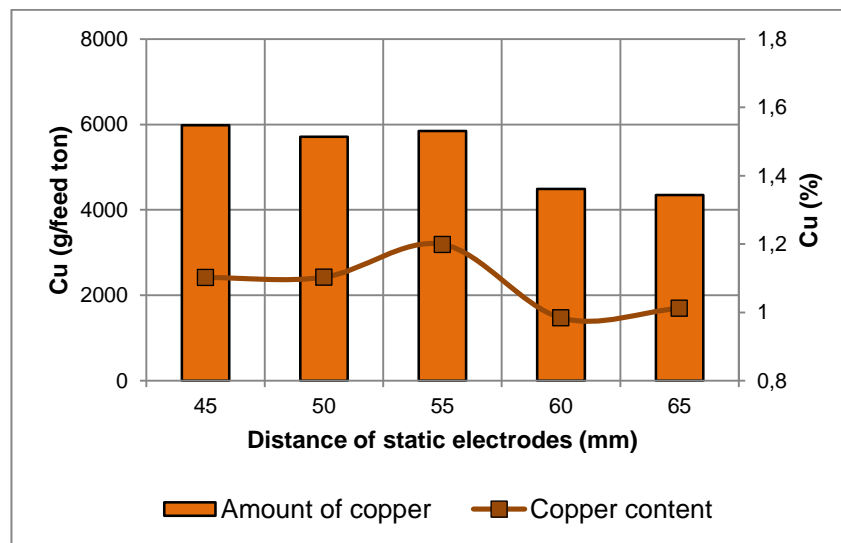


Figure 50 Effect of static electrode distance on content and amount of Cu in product

As Figure 49 shows, the distance of static electrodes from the roll slightly affects to the mass fractions of product and middling; when the distance is raised 20 mm, the mass fraction of product decreases and the mass fraction of middling increases approximately 13 percentage points. With the distance of 55 mm the mass fractions of product and middling are almost the same. Figure 50 shows that the copper content of product is a

bit higher with the distance of 55 mm than with the other distances, but the difference is quite small; the difference between lowest and highest copper content is only 0,2 percentage points. The amount of recovered copper is approximately 1500 grams more with the distances of 45 to 55 mm, than with the higher distances.

8.1.5 Effect of divider distance

Figure 51 presents the effect of divider distance on output mass fractions and Figure 52 the effect on copper content in product and the amount of recovered copper.

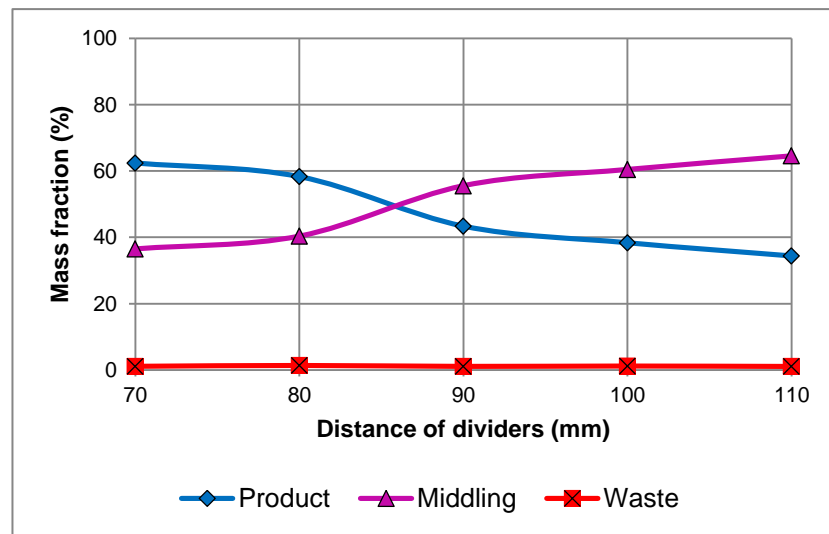


Figure 51 Effect of distance of dividers on output mass fractions

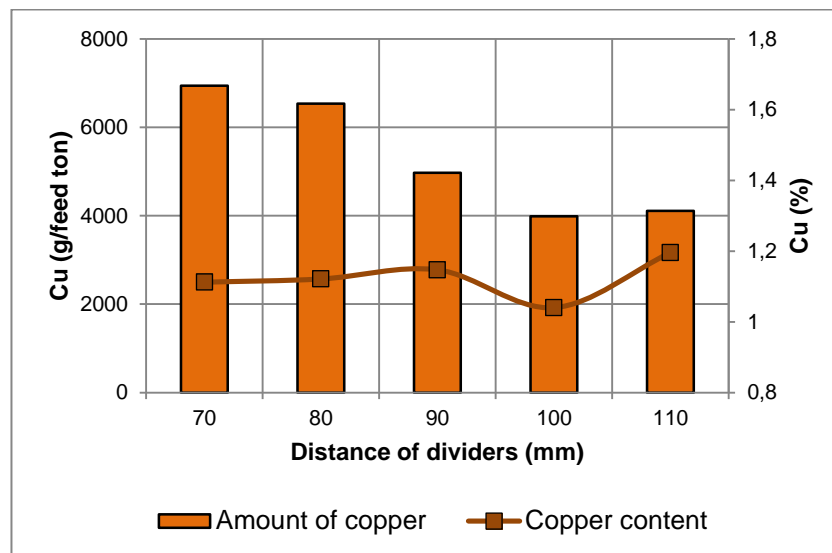


Figure 52 Effect of distance of dividers on Cu content and amount in product

As can be seen from Figure 51, when the distance of the dividers from the rotating roll is increased, the mass fraction of product decreases and the mass fraction of middling increases. With the distance of approximately 86 mm the mass fractions are the same. With smaller distances the fraction of product is higher than the fraction of middling, and with higher distances the other way around. Figure 52 shows that on the copper content of product the distance of dividers does not have significant effect; the content varies approximately between 1-1,2 %. Thus, the amount of recovered copper is highest when the mass fraction of product is highest.

8.2 Main experiments

The results of main experiments were analysed by examining the mass fractions of product and middling, the copper content of product and middling and the amount of recovered copper in product and middling. The copper content and amount in middling was added to the examination to investigate the ratio of product and middling copper contents. The purpose was also to find out which amount of the copper actually ends up to product and which to middling if one ton of material is fed to the separator. As in the preliminary experiments, the amount of copper describes the relationship of copper content in product/middling and the mass fraction of product/middling.

Precious metal contents were analysed with ICP-OES from two samples per experiment, because there was not enough resources to analyse more samples.

8.2.1 Tests to improve product quality

Figure 53 presents the effect of low voltage on output mass fractions and Figure 54 the effect of low voltage on copper content in product and in middling, and the amount of copper that ends up to product and middling with each voltage value if one ton of material is fed to the separator.

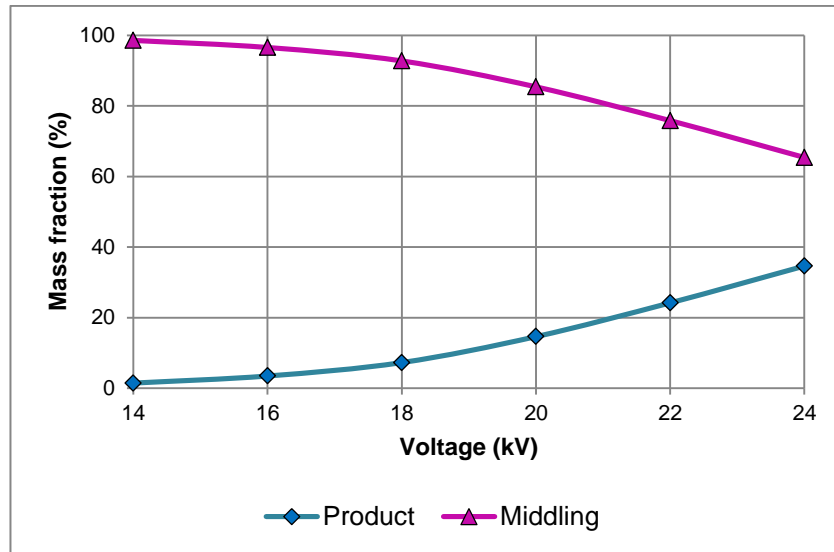


Figure 53 Effect of low voltage on output mass fractions

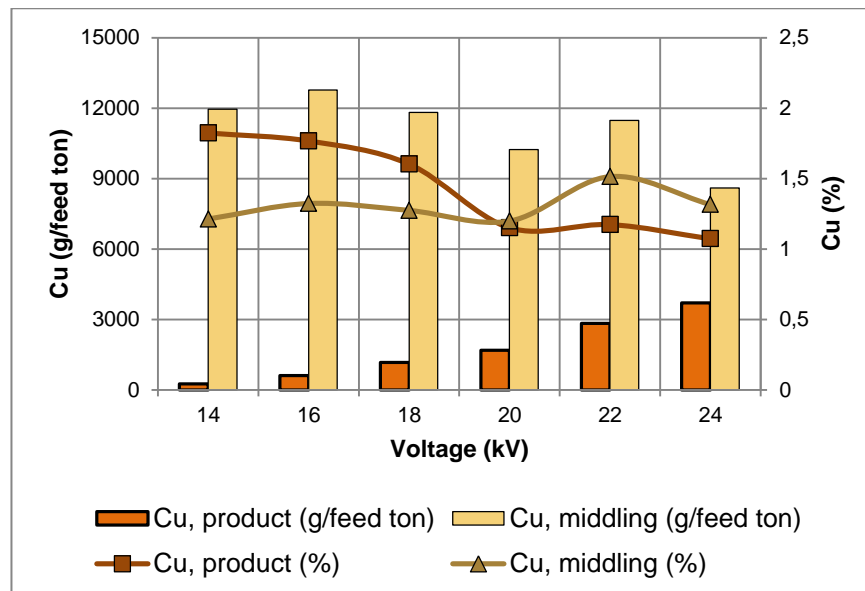


Figure 54 Effect of low voltage on content and amount of Cu in product and in middling

As can be seen from Figure 53, weak electric field causes the mass fraction of product to drop close to one percent when voltage is reduced to 14 kV, but it does not seem to significantly improve the selectivity of separator and product quality. Figure 54 shows that even with the voltage of 14 kV when the copper content of product is highest, the content of copper still stays under 2 %. The results also show that there is only a slight difference between the copper contents of product and middling despite the value of voltage. The amount of recovered copper is highest with the highest voltage, but still most of the copper ends up to middling.

Figure 55 presents the precious metal contents in product samples of voltages 14 kV and 18 kV.

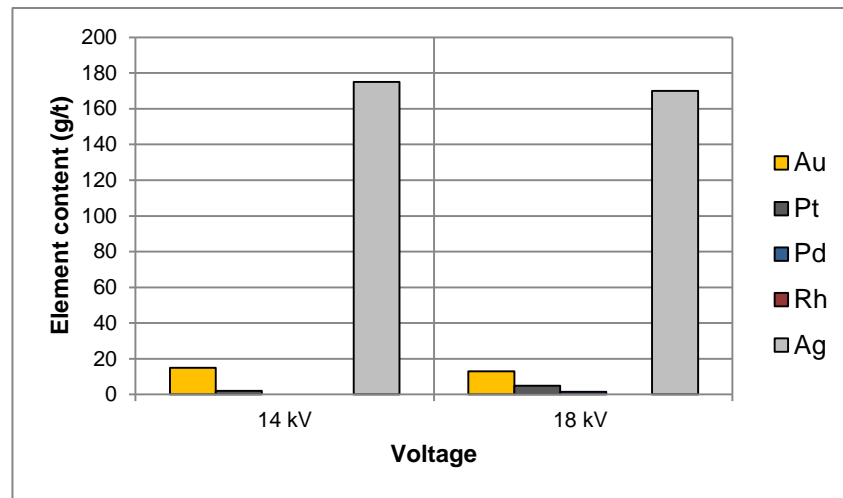


Figure 55 Effect of low voltage precious metal contents in product

As can be seen from Figure 55, the 4 kV difference in voltage has negligible effect on the precious metal content in product. However, silver seems to have enriched to the product, when comparing the silver contents of Figure 55 to the silver contents of F5 size fractions in Figure 23. In the size fractions of 0,25-2 mm the average silver content is approximately 80 g/t, and in the product samples of the main experiment 1 approximately 170 g/t.

The downside of low voltage is that a lot of impurities end up to the product. Figure 56 shows a sample of product with voltage of 14 kV and Figure 57 a sample of product with voltage of 24 kV.



Figure 56 Product sample with voltage of 14 kV



Figure 57 Product sample with voltage of 24 kV

In Figure 56 can be seen many small “sticks” that seem to be wooden. The sticks should not even be in the feed material, because wood would have burned in the incinerator. However, the origin of the sticks could not be found out. In addition, the sticks should not have ended up to the product because wood does not conduct electricity. As can be seen from Figure 57, the 24 kV product does not contain as much impurities as 14 kV product.

8.2.2 Effect of corona electrodes on product’s purity

In main experiment 2 tests were carried out to find out if the “sticks” that ended up to the product with low voltages would adhere to the surface of the rotating roll and end up to middling or waste with smaller distances of corona electrodes. Figure 58 shows a

photo of the product sample with corona electrode distance of 35 mm, and Figure 59 the product sample with distance of 65 mm.



Figure 58 Product sample with corona electrode distance of 35 mm



Figure 59 Product sample with corona electrode distance of 65 mm

As can be seen from Figure 58, lot of impurities ended up to product with also small distance of corona electrodes. When comparing Figure 58 to Figure 59 which presents the product with corona distances of 65 mm, no difference in the amount of impurities can be seen. Thus, the corona electrode distance does not seem to affect to product's purity.

Figure 60 and Figure 61 present the effect of corona electrodes with low voltage on product and middling mass fractions and on copper content and amount in product and in middling.

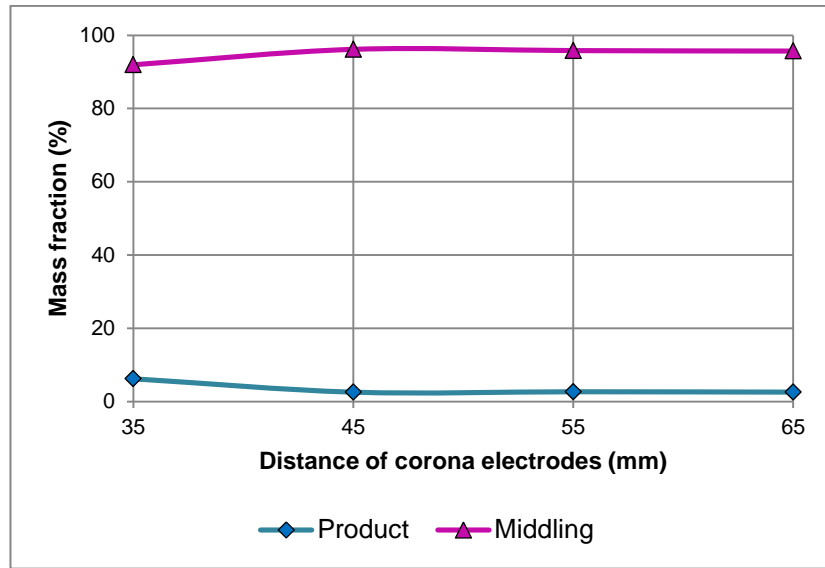


Figure 60 Effect of distance of corona electrodes on output mass fractions

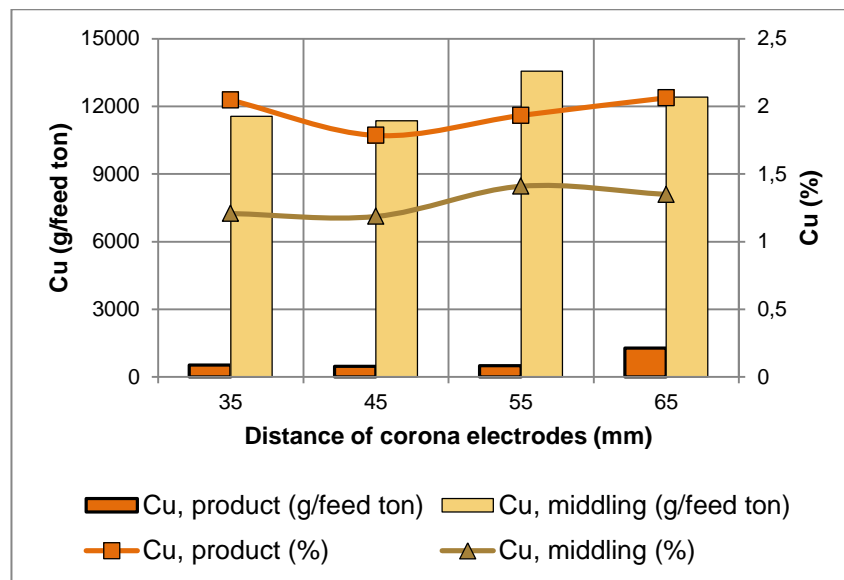


Figure 61 Effect of distance of corona electrodes on Cu content and amount in product and in middling.

Figure 60 demonstrates the same as Figure 47 in pre-experiments: The distance of corona electrodes has a negligible effect on the mass fractions of product and middling, especially with the low voltage. Also the effect on copper content of product and middling is very minor, as Figure 61 shows, and thus also the effect on the amounts of copper. Instead, the distance of corona electrodes seems to have an effect on the precious metal contents in product. Figure 62 presents the precious metal content of

product with short and long distances of corona electrodes. With the distance of 65 mm the contents of precious metals are higher than with the distance of 35 mm.

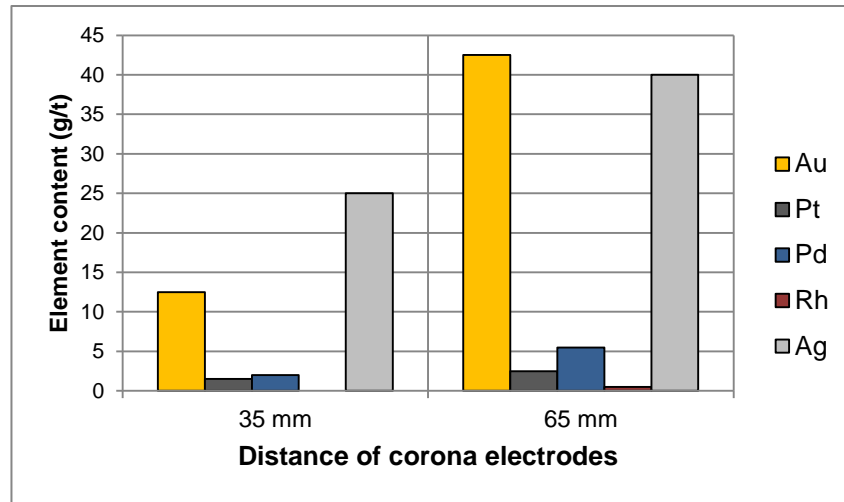


Figure 62 Effect of corona electrode distance on product's precious metal contents

8.2.3 Factor experiments

The purpose in factor experiments was to investigate the effect of different combinations of variable values on the separation, and also the effect of rotor impact mill. Table 16 presents the variable values used in each test to ease the interpretation of the figures. The effect of rotor impact mill can be analysed by comparing the results of F5 and F12, from which F12 has gone through the rotor impact mill and F5 has not.

Table 16. Variable values in factor experiments.

Test nro	Voltage (kV)	Distance of dividers	Distance of corona electrodes
1	22	11	60
2	22	11	50
3	22	7	60
4	22	7	50
5	16	11	60
6	16	11	50
7	16	7	60
8	16	7	50

Figure 63 and Figure 64 present the mass fractions of product and middling in each test with material F5 and F12.

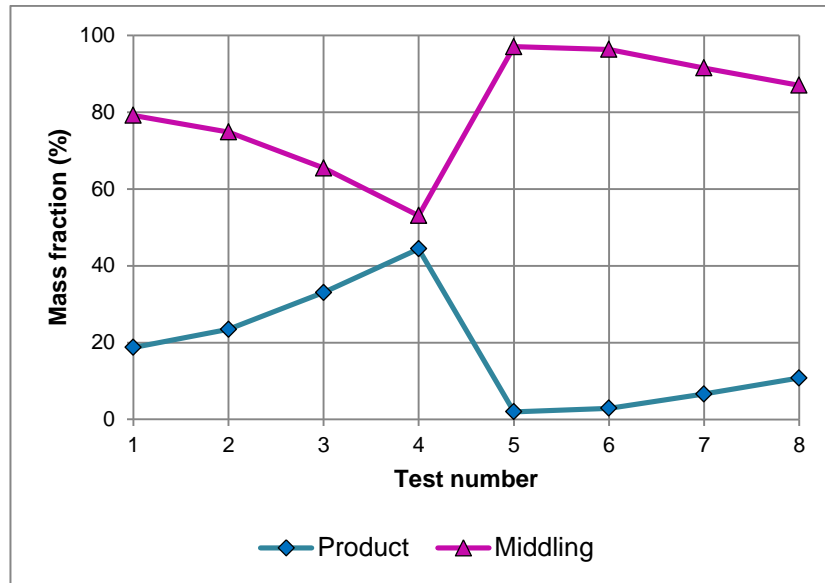


Figure 63 Material F5, effect of different combinations of variables' values on output mass fractions

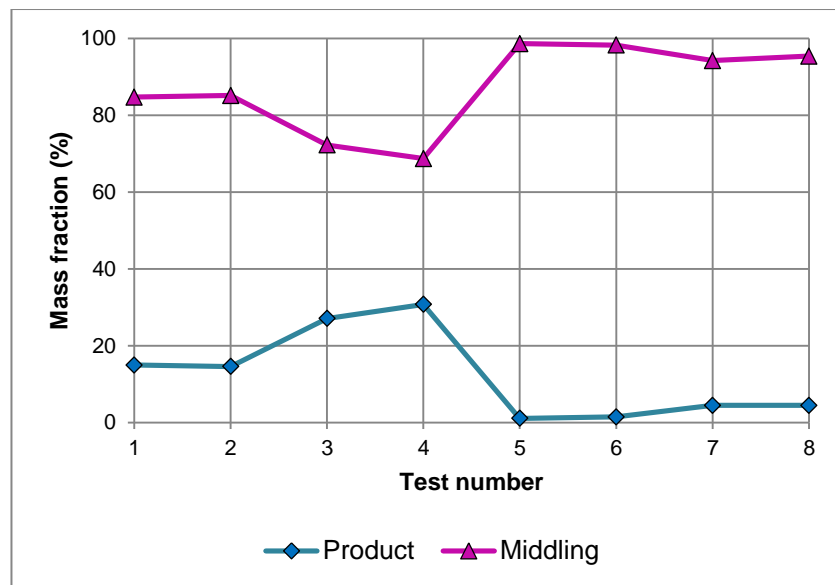


Figure 64 Material F12, Effect of different combinations of variables' values on output mass fractions

Figure 63 and Figure 64 show that with higher voltages the mass fraction of product is higher than with lower voltages, if compared the results from tests 1-4 and 5-8. By comparing the tests 1 and 2, and 5 and 6 can be seen that the 10 mm shorter distance between roll electrodes and corona electrodes does not really have an effect on the mass fractions when distance of the dividers is 11 mm, but when the distance of the dividers is 7 mm the shorter distance of corona electrodes raises the mass fraction of product a

bit. By comparing the tests 1 and 3, and 5 and 7, can be seen that the lower distance of dividers raises the amount of product, and the change in the mass fractions is bigger with higher voltage. Highest the mass fraction of product is with higher voltage and shorter distances of corona electrodes and dividers.

Figure 65 and Figure 66 present the copper contents and amounts of copper in product and in middling.

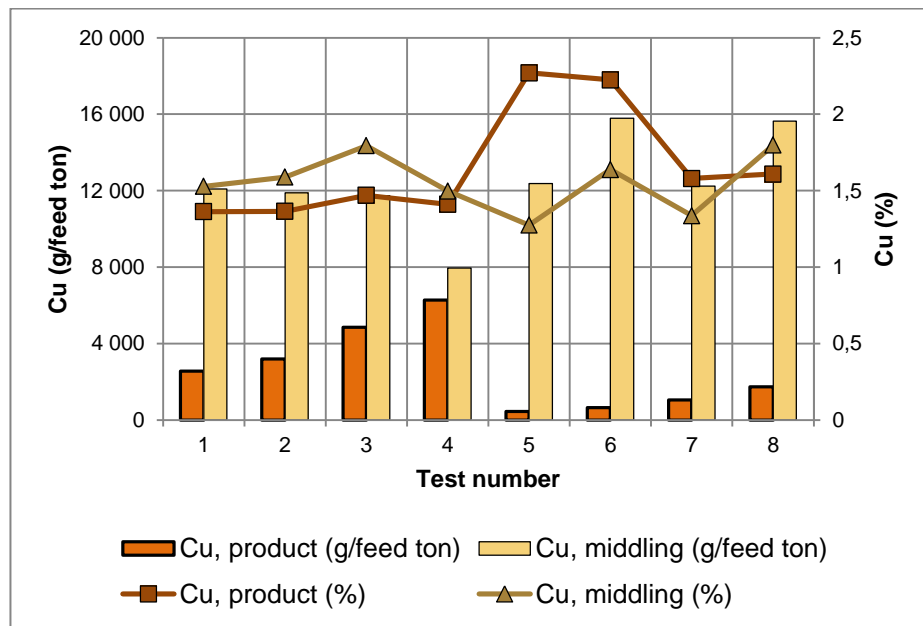


Figure 65 Material F5, effect of different combinations of variables' values on Cu content and amount in product and in middling

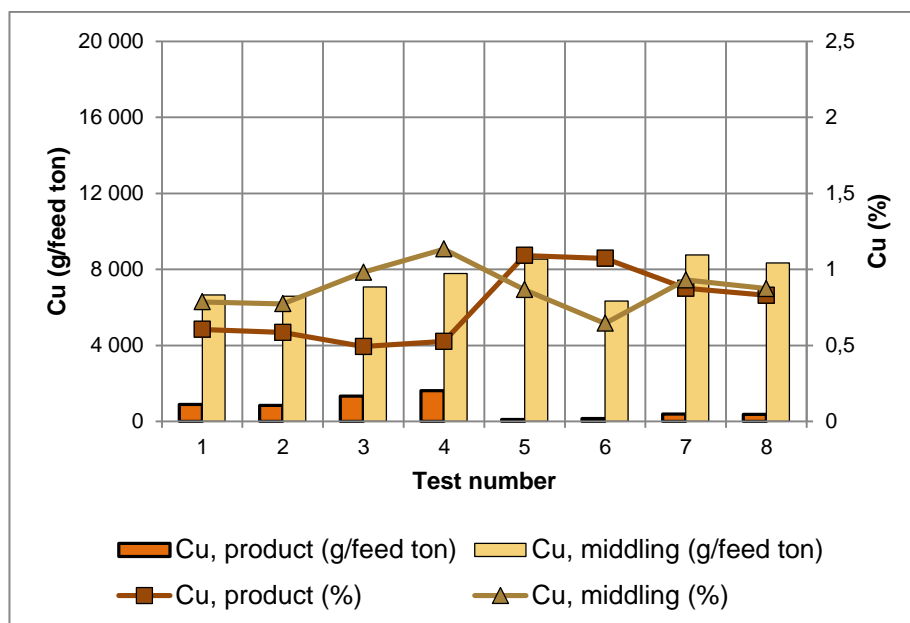


Figure 66 Material F12, effect of different combinations of variables' values on Cu content and amount in product and in middling

Figure 65 and Figure 66 show that the copper content of product is higher with the lower voltage than with the higher voltage, but the amount of recovered copper is much smaller because of the small mass fraction of product. The content is highest in product with lowest voltage and longest distances, while the amount of copper in product is highest with highest voltage and lowest distances. The distance of corona electrodes does not really have an effect on the copper contents and amounts, but the change in the distance of dividers from 110 mm to 70 mm seems to lower a bit the copper content of product.

Precious metal contents were analysed with ICP-OES from product samples of tests 4 and 5. Tests 4 and 5 were chosen because according to the Figures 63-66, the results of those tests differed most from each other and the effect of the change in variable values on the precious metal contents was found interesting to investigate. Variable values of tests 4 and 5 are presented in Table 17. Figure 67 presents the results of material F5, and Figure 68 the results of material F12.

Table 17 Variable values of tests 4 and 5

Test nro	Voltage (kV)	Distance of dividers (mm)	Distance of corona electrodes (mm)
4	22	70	50
5	16	110	60

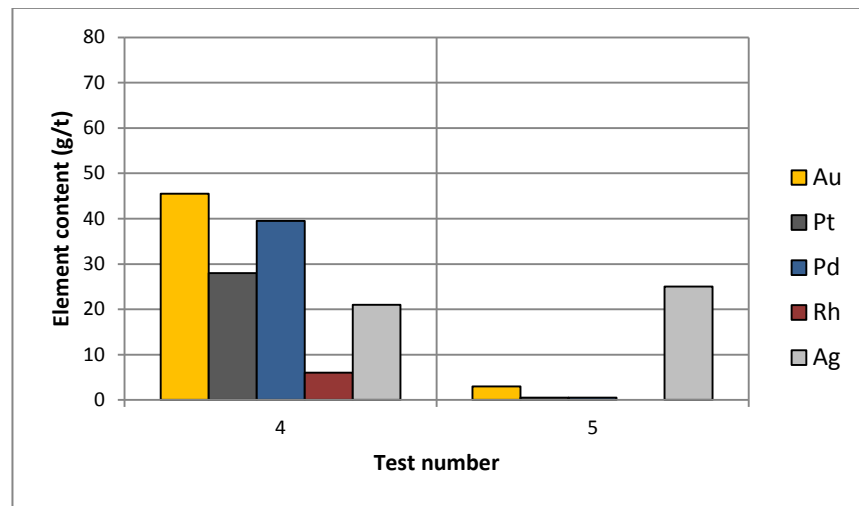


Figure 67 Material F5, effect of variable combinations on product's precious metal contents

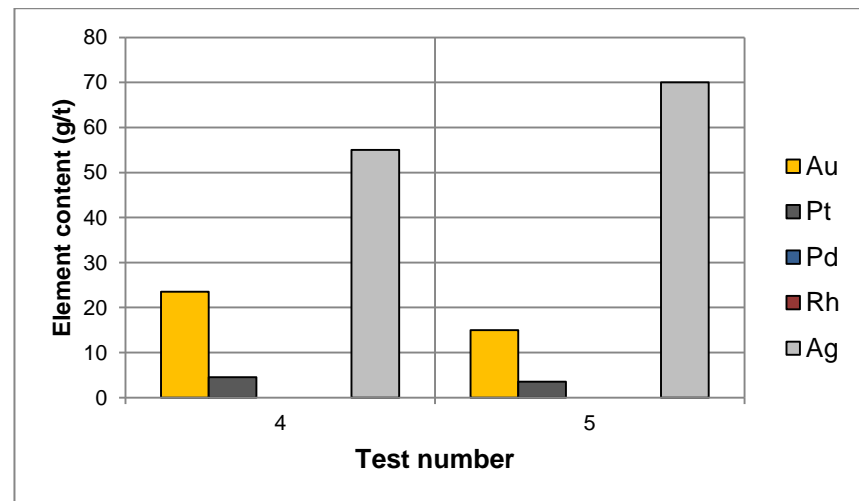


Figure 68 Material F12, Effect of variable combinations on product's precious metal contents

As can be seen from Figure 67 and Figure 68, the change in variable values has the same kind of an effect on gold and silver contents in both materials: when voltage is decreased and the distances of corona electrodes and dividers increased, the content of silver slightly increases in the product, but the content of gold decreases. One possible

reason for the results could be the better electric conductivity of silver compared to gold: theoretically silver particles would “fly” slightly further than gold particles because they are affected more by the electric field. When the voltage is decreased and the distance of dividers increased, less gold particles and other particles end up to the right side of the divider to the product, which leads to the increase in product’s silver content and decrease in gold content.

Effect of rotor impact mill

As can be seen from Figure 63 and Figure 64, the shapes of the curves in both figures are almost the same, indicating that the changes in variable values affect in the same way to both materials. The biggest difference is the distance between product and middling curves: with the material F12 the curves are further away from each other than with F5. This means that the rotor impact mill has a negative effect on the separation in a way that the mass fraction of product is smaller.

The examination of Figure 65 and Figure 66 reveals that the copper content in product and middling, as well as the amount of copper in product and middling, are lower with material F12 than with material F5. Instead, according to Figure 67 and Figure 68, the mill seems to have positive impact on the silver content of product.

8.3 Additional experiments

The purpose of additional experiments was to investigate the effect of feed rate, moisture, dust and distance of upper divider on the separation. The results were analysed through the particles’ distribution to product and middling, and through the copper contents and amounts in product and middling. In the experiment related to feed rate also the capacity with different feed rates was calculated.

8.3.1 Effect of feed rate

Figure 69 presents the effect of feed rate on product and middling mass fractions and Figure 70 on copper content and amount in product and in middling.

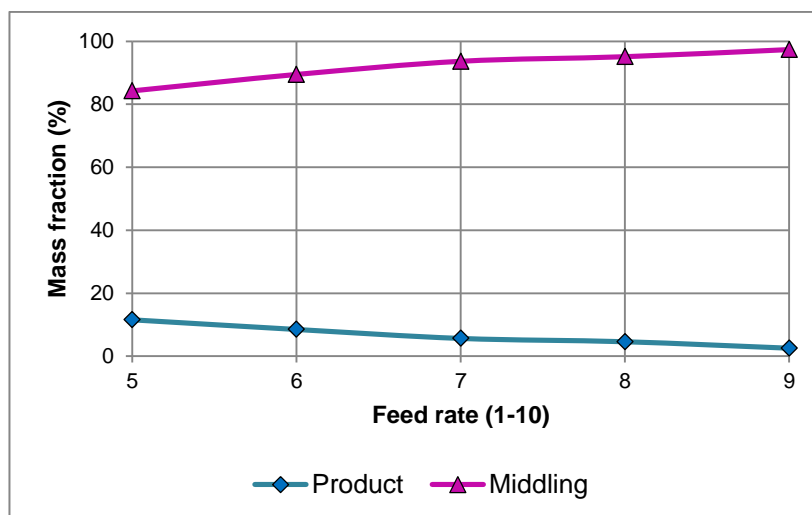


Figure 69 Effect of feed rate on output mass fractions

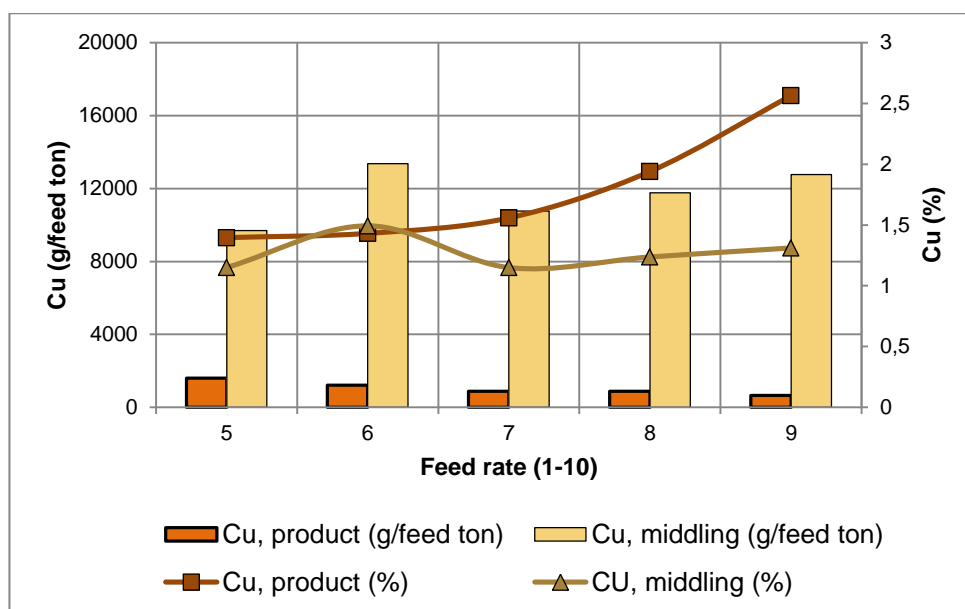


Figure 70 Effect of feed rate on Cu content and amount in product and middling

Figure 69 shows that increase in feed rate lowers the mass fraction of product and increases the mass fraction of middling. From Figure 70 can be seen that the copper content of product increases when feed rate is increased, but on the copper content of middling the changes in feed rate do not have that much impact. The amount of copper in product is biggest with the feed rate 5, but the difference between the recovered copper with feed rates 5 and 9 is quite small, less than 1000 grams per ton. As can be seen, the amount of copper in middling is many times bigger than the amount of copper in product with all the feed rates.

Precious metal contents in product with feed rates 5 and 9 are presented in Figure 71.

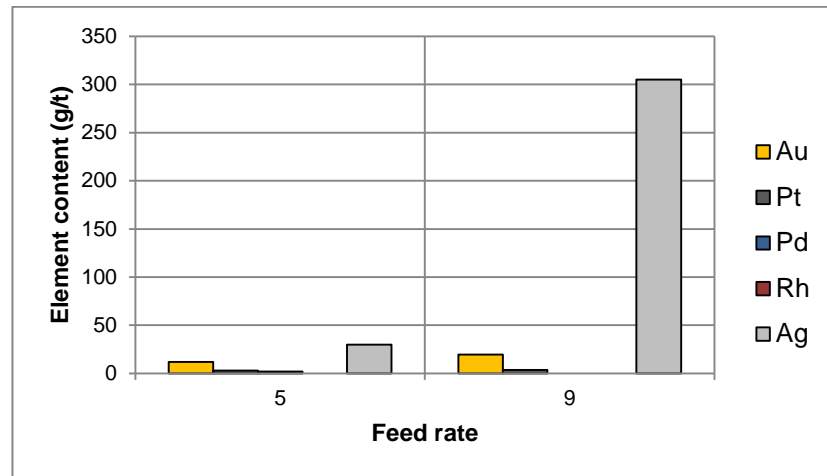


Figure 71 Effect of feed rate on precious metal contents in product

According to Figure 71 silver content in product increases significantly, when feed rate is increased from 5 to 9. Instead the effect of feed rate to other precious metal contents is very minor. However, it seems to be advantageous to run the separation with high feed rate.

Capacity

Figure 72 presents the effect of feed rate on electrostatic separator's capacity. As can be seen, the capacity grows very rapidly when feed rate is increased. With feed rate 5 the capacity is only approximately 11 kg/h, but with feed rate 7 already approximately 110 kg/h and with feed rate 9 even approximately 680 kg/h.

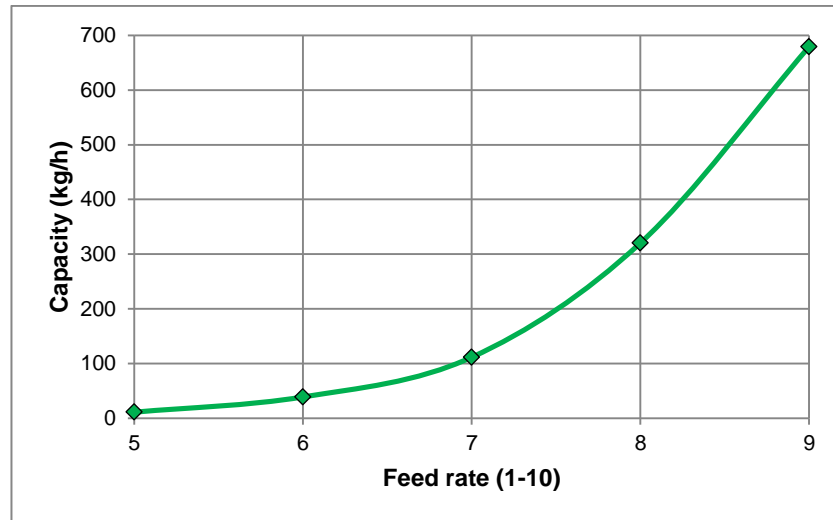


Figure 72 Effect of feed rate on capacity

8.3.2 Effect of upper divider distance

Figure 73 presents how the distance of upper divider from the roll electrode affects to the mass fractions of product and middling, and Figure 74 shows the changes in copper content and amount in product and in middling.

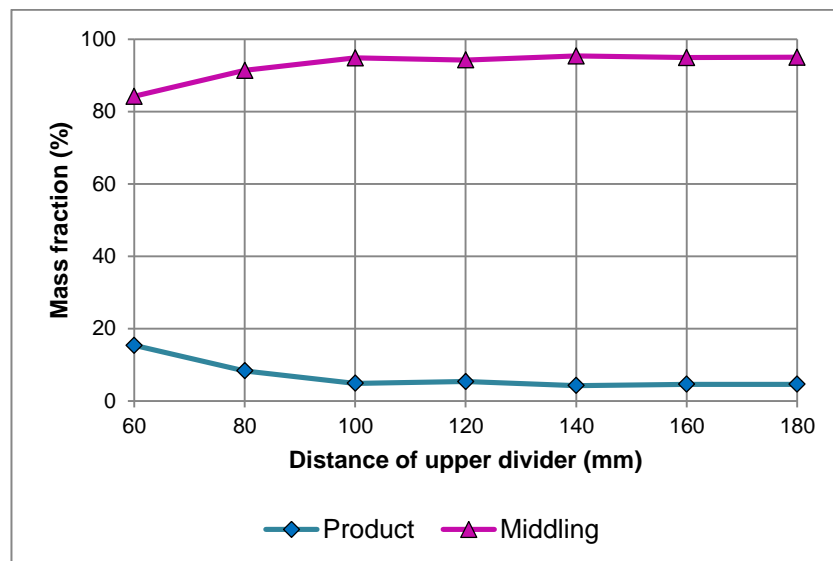


Figure 73 Effect of upper divider on output mass fractions

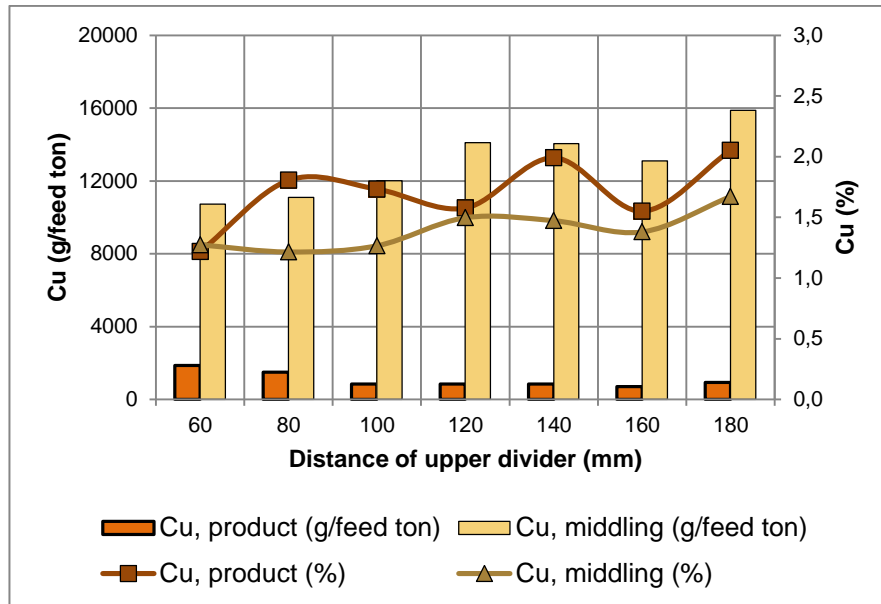


Figure 74 Effect of upper divider on content and amount of Cu in product and in middling

Figure 73 shows that from 60 mm to 100 mm the mass fraction of product decreases and the mass fraction of middling increases when the distance of dividers is grown, but after the 100 mm, increase in the distance does not seem to have an effect on the mass fractions anymore. According to Figure 74 the copper content does not seem to follow any certain logic related to the distance of upper divider; more investigations would be required for more accurate analysis.

Figure 75 presents the effect of upper divider distance on precious metal contents in product.

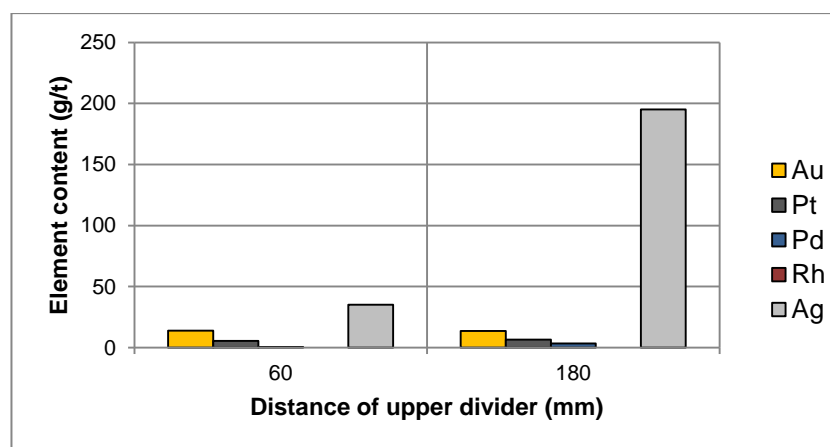


Figure 75 Effect of upper divider distance on precious metal contents in product

As can be seen from Figure 75, three times longer distance between upper divider and roll electrode increases significantly silver content in product, but does not seem to affect to the contents of other precious metals. However, according to the results of only two samples it is impossible to say whether there is a clear trend between increasing distance and increasing silver content, or whether the silver content acts as randomly as copper content.

8.3.3 Effect of moisture

The effect of moisture was investigated by carrying out tests 4, 5 and 8 from the factor experiments with un-dried F12 material and comparing the results to the results of factor experiment carried out with dried F12 material. The un-dried material used in this experiment has come from different plant than the dried material used in factor experiment, so the values of copper contents and amounts in dry and moist material cannot be compared with each other. Instead, the effect of changes in variable values on the mass fractions and copper and content and amount in product and middling can be compared, as well as precious metal contents in product. This comparison reveals whether the changes affect in the same way to the separation with dry and moist material.

The variable values used in the tests are presented in Table 18 below.

Table 18. Variable values used in the tests.

Test nro	Voltage (kV)	Distance of dividers	Distance of corona electrodes
1	22	7	50
2	16	11	60
3	16	7	50

Figure 76 presents the effect of moisture on output mass fractions.

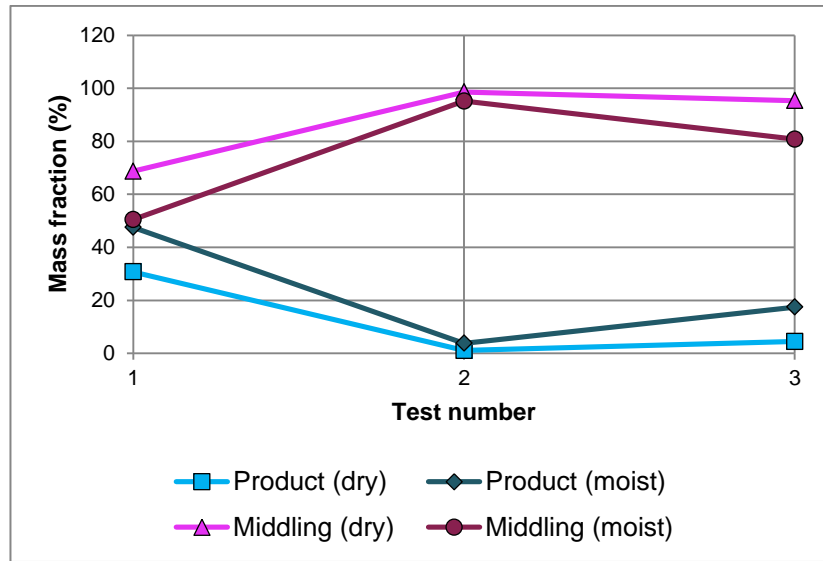


Figure 76 Effect of moisture on output mass fractions

Figure 76 shows that the mass fractions of dry and moist material behave in the same way when the values of the variables are changed; the change in the mass fractions is only a bit bigger in the case of moist material.

Figure 77 presents the effect of moisture on copper content and amount in product, and Figure 78 in middling.

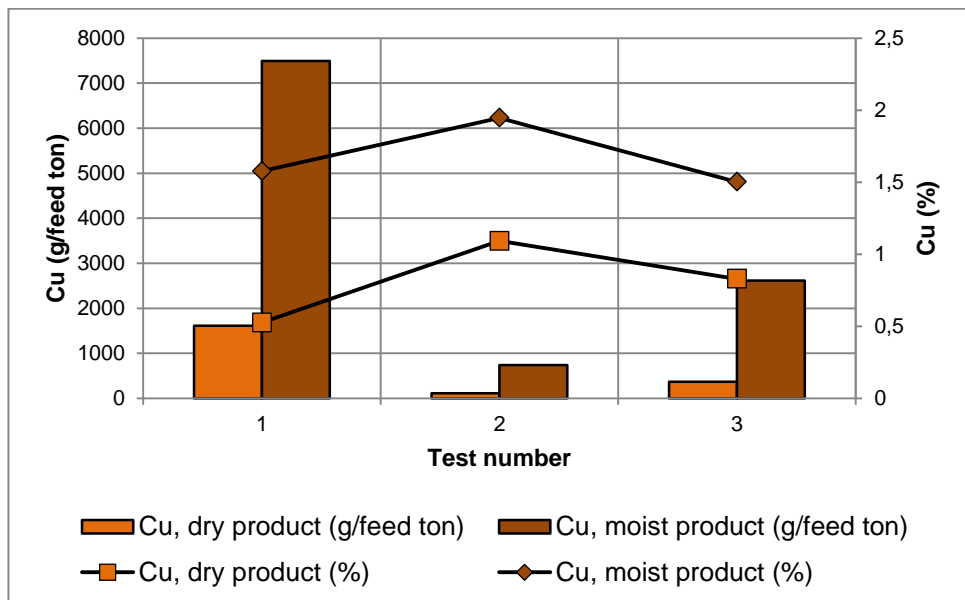


Figure 77 Effect of moisture on Cu content and amount in product

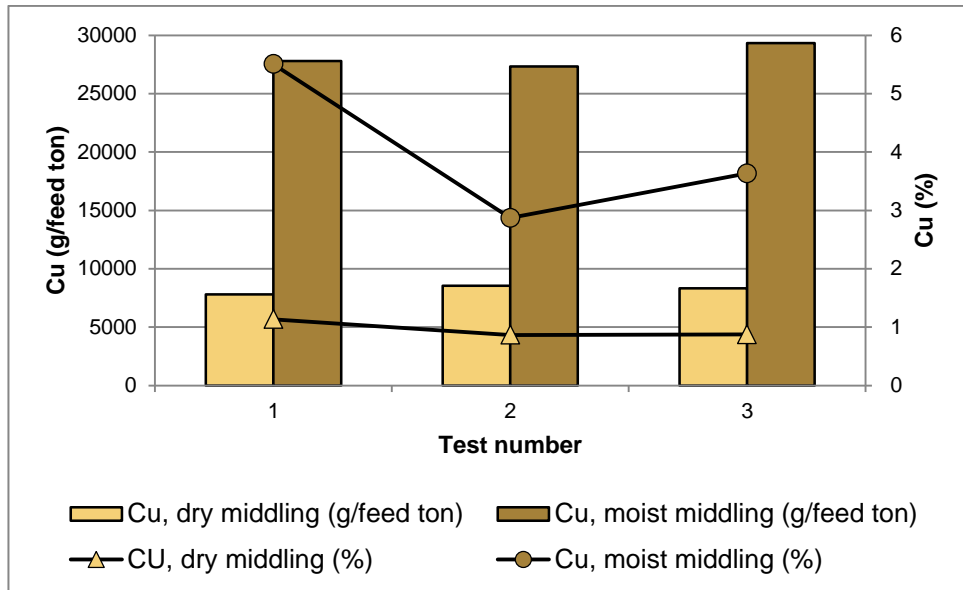


Figure 78 Effect of moisture on Cu content and amount in middling

As can be seen from Figure 77 and Figure 78, the copper contents and amounts of dry and moist materials act mostly in the same way. Only between copper contents of dry and moist middling can be seen clear difference between the shapes of the curves: the content of moist middling varies more than the content of dry material.

Figure 79 presents the precious metal contents of product in moist and dry materials with the same variable values.

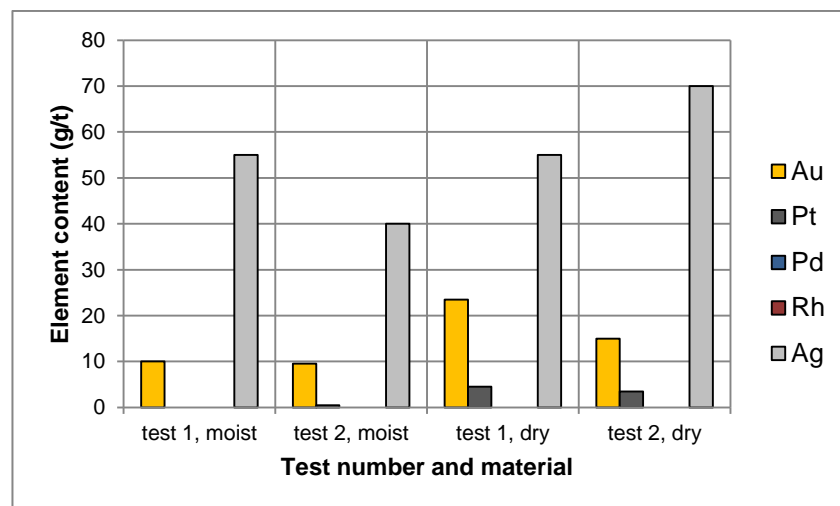


Figure 79 Effect of variable combinations on product's precious metal contents in moist and dry materials

As can be seen from Figure 79, the precious metal contents act differently in moist and dry materials. In moist material the lower voltage and longer distances of corona electrodes and dividers cause the silver content to drop, whereas in dry material the silver content rises. Gold content in moist material does not change when the variables are changed, but in dry material the content of gold in product decreases with lower voltage and longer distances.

8.3.4 Effect of dust

Effect of dust was investigated in the same way as effect of moisture, but instead of using moist material, the tests were carried out with dry F12 material with size range of 0-2 mm. Three tests were carried out with variable values presented in Table 18 and the test results were compared with results from factor experiment. The material used in the tests came from the same company as the material used in factor experiment, which means that unlike in the case of moist material, also the copper contents and amounts of the test material as well as precious metal contents of product can be compared with the results of 0,28-2 mm material.

Figure 80 shows the effect of dust on mass fractions of product and middling.

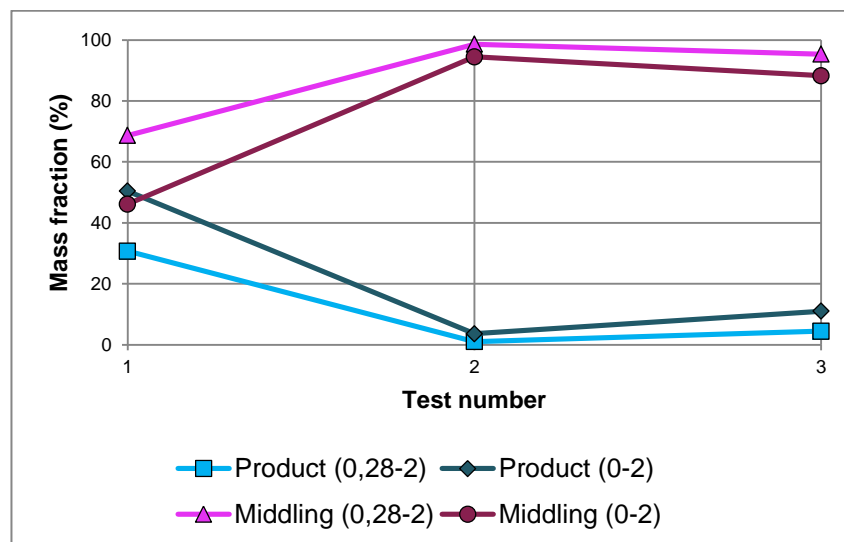


Figure 80 Effect of dust on output mass fractions

In test 1 the mass fraction of product with size range of 0-2 mm is higher than the fraction of 0,28-2 mm product, but in the tests 2 and 3 no significant difference appears between the two materials.

From Figure 81 and Figure 82 can be seen the copper contents and amounts of the two materials in product and in middling.

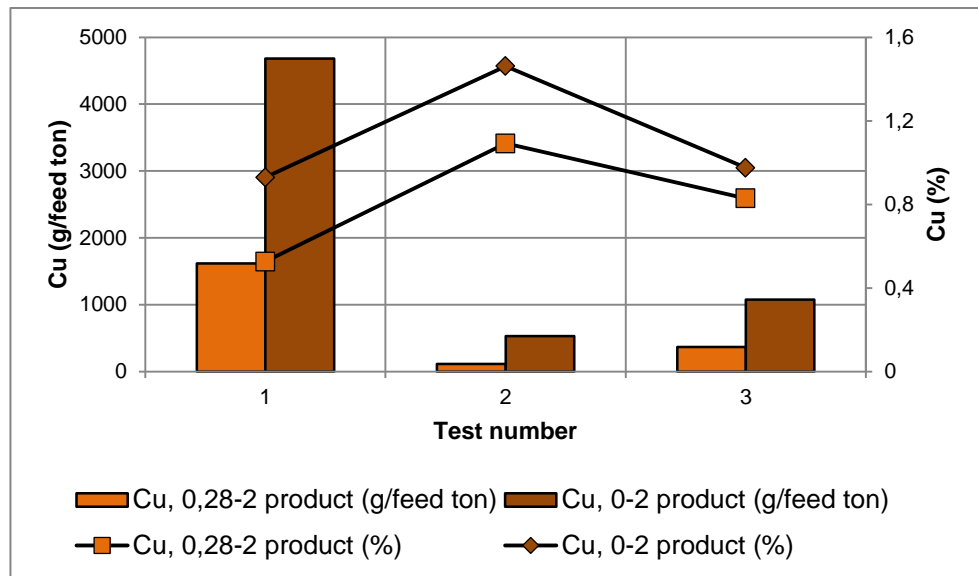


Figure 81 Effect of dust on Cu content and amount in product

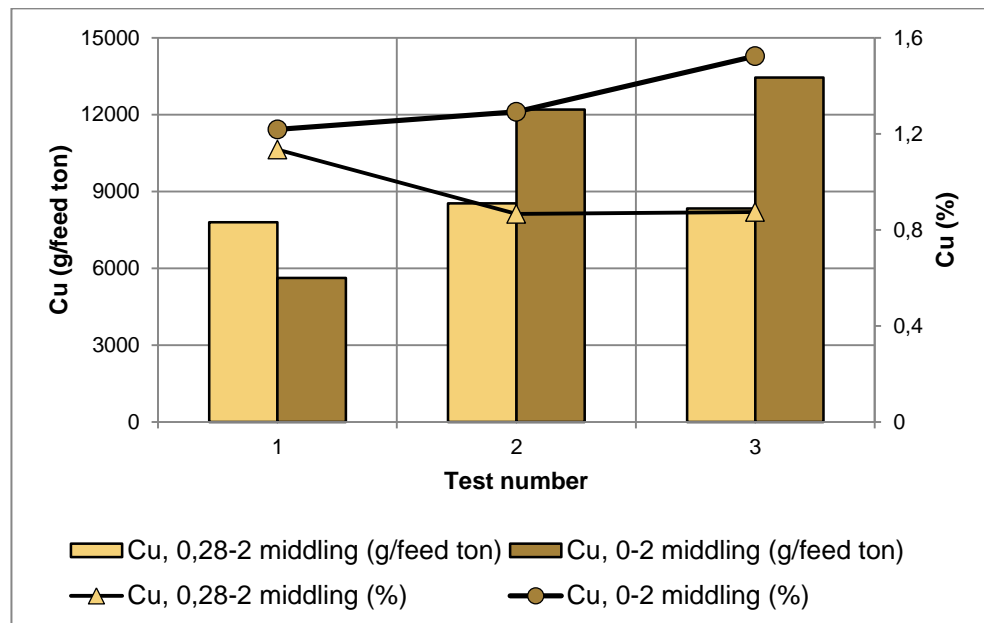


Figure 82 Effect of dust on Cu content and amount in middling

Figure 81 shows that the change in variable values has the same effect on both materials' copper contents and amounts in product. The difference is that the copper content is higher with 0-2 mm material, and thus also the amount of recovered copper.

Figure 82 shows that there is a difference in how the copper contents of middlings act in different tests. With lower voltage the copper content of 0,28-2 mm middling clearly decreases, while the content of 0-2 mm middling stays almost the same, or even increases. In the test 1 the copper contents are almost the same.

Figure 83 presents the precious metal contents in material with dust and in material without dust in tests made with same parameter values.

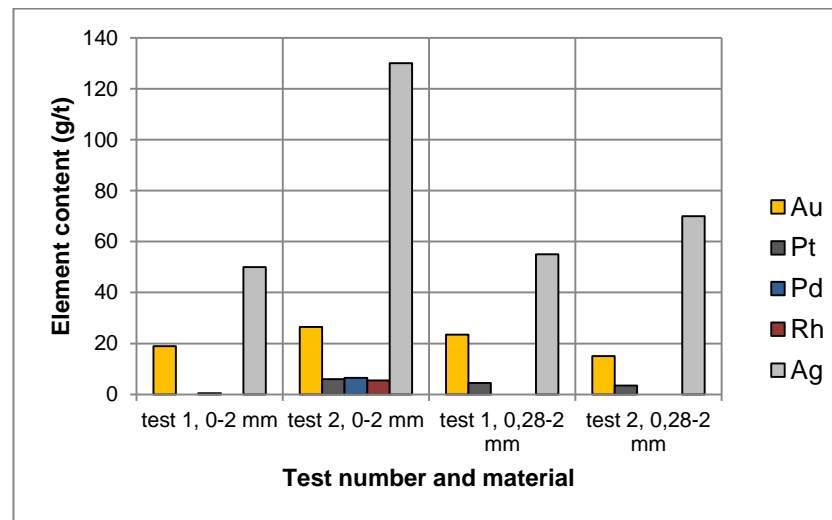


Figure 83 Effect of variable combinations on product's precious metal contents in material with dust and in material without dust.

As can be seen from Figure 83, lower voltage and longer distance of corona electrodes and dividers increase the silver content of product in both materials; in material with dust also the content of gold. In test 1 the precious metal contents of product are higher in material without dust, but in test 2 the contents are higher in material with dust.

Because the recovered amount of copper in product is so much higher with 0-2 mm material than with 0,28-2 mm material, and in the test 2 also the contents of precious metals are higher with 0-2 mm material, it seems that at least with F12 material it is beneficial to drive also the most finest material through the separator.

Conclusions

The applicability of corona electrostatic separator on the separation of fine metal fraction of MSWI bottom ash was investigated. Objective was to find out if copper and precious metals could be enriched to the product in the output, and investigate the effect of equipment parameters on the separation.

In preliminary experiments the effect of voltage, roll speed, distance of corona electrodes, distance of static electrodes and distance of dividers on the separation were investigated. From these parameters voltage had the most significant effect on the output mass fractions: the mass fraction of product dropped from 41 % to 13 % when voltage was reduced from 28 kV to 20 kV. Change in roll speed caused only couple of percents variation in mass fractions. Increase in the distances of corona electrodes, static electrodes and dividers lead to decrease in product mass fraction and increase in middling mass fraction.

None of the parameters had an effect on the mass fraction of waste which stayed below 2 % in every test. Also the effect of the parameters on copper content in product was minor: the content of copper varied between 1-1,7 % throughout the tests. The highest contents were reached with low voltages and high roll speeds. Between the distances of corona electrodes, static electrodes and dividers and the copper content of product could not be seen any clear correlation.

Due to the small copper content of product in pre-experiments, the main experiment 1 focused on investigating the possibility of improving the selectivity of the separator by creating weak electric field. However, the weak electric field did not prevent the least conductive particles ending up to product, and the highest copper content of product was only 1,8 %. Overall, the results of main experiments indicated that low voltage (16 kV) and long distance between the dividers and roll electrodes (110 mm) slightly increase copper and silver contents in product compared to a higher voltage (22 kV) and shorter distance of dividers (70 mm), but significantly decrease the mass fraction of product, which leads to very small amounts of recovered copper and silver. Contents of other precious metals, especially gold, seem to be a bit higher with higher voltage and shorter distances. The effect of the distance of corona electrodes on the output mass

fractions and copper contents was detected to be very minor, but in main experiment 2 the long distance (65 mm) increased the precious metal contents in product compared to a short distance (35 mm).

In additional experiments higher feed rate resulted in higher copper and silver contents of the product. The equipment worked well with also the feed rate 9 (scale from 1-10) which was the highest feed rate tested, but produced so much dust that more efficient dust removal system should be considered if running the equipment with that high feed rate. The change in the distance of upper divider had a varying effect on the copper content, but it seems that with high distances the content is on average slightly higher than with shorter distances. Instead, the silver content of product increases significantly when the distance of upper divider is grown from 60 to 180 mm.

Moisture content of the material does not seem to have significant effect on the separation: the output mass fractions and copper content of product act in the same way as in dried material when parameter values are changed. The changes in precious metal contents of product are also quite minor. The material with dust acts in the same way as material without dust, but the copper contents in product and in middling in material with dust are slightly higher. With low voltage and long distances of dividers and corona electrodes the silver content of product in material with dust is significantly higher as in material without dust, but the difference in other precious metal contents is minor.

Maximum copper content in the product was 2,6 %. Silver and gold contents in product varied between 21-305 g/t and 3-46 g/t, respectively. In most of the analysed product samples rhodium content was 0 g/t and platinum and palladium contents 0-6 g/t. Thus, some enrichment of precious metals to the product has happened in some of the tests, but it should be taken into account that relatively small amount of the samples were finally analysed for the precious metal contents. More research would be needed for accurate conclusions about the enrichment of precious metals.

Processing of the material in rotor impact mill weakens the separation efficiency in a way that with same variable values the mass fraction of middling is bigger compared to material that has not been processed in the mill, and also the copper content of product

is lower in the processed material. However, the mill seems to have positive effect on the silver content of product.

To sum up, according to the results of the experiments can be concluded that corona electrostatic separator is not applicable for the test material. The equipment itself works and it separates the material stream into three fractions, but its selectivity is not enough for the metal fraction of MSWI bottom ash. For the separation of some other fine granular mixture with larger differences in conductivities the corona electrostatic separator could be suitable; for example for crushed waste printed circuit boards.

References

Allegrini, E., Maresca, A., Olsson, M. et al. 2014. Quantification of the resource recovery potential of municipal solid waste incineration bottom ashes. *Waste Management*, not yet published. Available: <http://dx.doi.org/10.1016/j.wasman.2014.05.003>.

Aubert, J.E., Husson, B. and Sarramone, N. 2006. Utilization of municipal solid waste incineration (MSWI) fly ash in blended cement – Part 1: Processing and characterization of MSWI fly ash. *Journal of Hazardous Materials B*, vol 136:3. P. 624-631. ISSN 0304-3894.

BHS. 2014. Rotor impact mill. [Web document]. [Referred 2.10.2015]. Available: <http://www.bhs-sonthofen.de/en/products/recycling-technology/rotor-impact-mill.html>

Chandler, A., Eighmy, T., Hatrlen, J. et al. 1997. Municipal solid waste incinerator residues. *Studies in Environmental Science*, vol 67. Elsevier 1997. ISBN 978-0-444-82563-6.

Chang, J., Kelly A. and Crowley. J. 1995. *Handbook of Electrostatic Processes*. New York, USA: Marcel Dekker, Inc. 763 p. ISBN 0-8247-9254-8.

Chimenos, J.M., Segarra, M., Fernández, M.A. and Espiell, F. 1999. Characterization of the bottom ash in municipal solid waste incinerator. *Journal of hazardous materials A*, vol 64:3. P. 211-222. ISSN 0304-3894.

Cui, J., Forssberg, E. 2003. Mechanical recycling of waste electric and electronic equipment: a review. *Journal of Hazardous Materials B*, vol 99:3. P. 243-263. ISSN 0304-3894.

Dascalescu, L., Morar, R., Iuga, A., Samuila, A. and Neamtu, V. 1998. Electrostatic separation of insulating and conductive particles from granular mixes. *Particulate Science and Technology*, vol. 16:1. ISSN 0272-6351.

Dascalescu, L., Samuila, A., Iuga, A., Morar, R. and Csorvasy, I. 1994. Influence of material superficial moisture on insulation-metal electroseparation. *IEEE Transactions on industry applications*, vol 30:4. ISSN 0093-9994.

Ekokem. 2014. Westenergy Oy Ab, Mustasaaren jätteenpolttolaitoksen kattilatuhka ja savukaasunpuhdistusjäte – Selvitys tuhkien ominaisuuksista ja haitallisuudesta ympäristölle. [Web document]. [Referred 5.6.2014]. Available: <http://www.westenergy.fi/img/Selvitys%20tuhkien%20ominaisuuksista.pdf>.

Higashiyama, Y. and Asano, K. 1998. Recent progress in electrostatic separation technology. *Particulate Science and Technology*, vol 16:1. P. 77-90. ISSN 0272-6351.

Hjelmar, O. 1996. Disposal strategies for municipal solid waste incineration residues. *Journal of Hazardous Materials*, vol. 47:1-3. P. 345-368. ISSN 0304-3894.

Integrating Research and Education. 2014. Scanning Electron Microscope. [Web document]. [Referred 26.9.2014].

International Ash Working Group (IAWG): Chandler, A.J., Eighmy, T.T., Hartlén, J. et al. 1997. *Municipal solid waste incineration residues*. Amsterdam. ISBN 0-444-82563-0.

ISWA, International Solid Waste Association – Working Group on Thermal Treatment of Waste, Subgroup on APC Residues from W-t-E Plants. 2008. *Management of APC residues from W-t-E Plants – An overview of management options and treatment methods*. [Web document]. [Referred 5.6.2014]. Available: http://www.iswa.org/uploads/tx_iswaknowledgebase/Management_of_APC_residues_from_W-t-E_Plants_2008_01.pdf.

Jätelaitosyhdistys. 2014. Arinapoltto. [Web document]. [Referred 27.5.2014]. Available: <http://www.jly.fi/energia31.php?treeviewid=tree3&nodeid=31>.

Kaartinen, T., Laine-Ylijoki, J., Koivuhuhta, A. et al. 2010. *Pohjakuonan jalostus uusiomateriaaliksi*. Espoo. VTT Tiedotteita. 98 p. ISBN 978-951-38-7679-1.

Kaartinen, T., Laine-Ylijoki J. and Wahlström M. 2007. *Jätteen termisen käsittelyn tuhkien ja kuonien käsittely- ja sijoitusmahdollisuudet*. [Web document]. [Referred 5.6.2014]. Available: <http://www.vtt.fi/inf/pdf/tiedotteet/2007/T2411.pdf>.

Laine-Ylijoki, J., Mroueh, U-M., Vahanne, P., Wahlström, M., Vestola E., Salonen S. and Havukainen J. 2005. *Yhdyskuntajätteen termisen käsittelyn kuonista ja tuhkista*

hyötykäytettäviä ja loppusijoitettavia tuotteita – kansainvälinen esiselvitys. [Web document]. [Referred 5.6.2014]. Available: <http://www.vtt.fi/inf/pdf/tiedotteet/2005/T2291.pdf>.

Lam, C., Ip, Alvin., Barford, J.P. and McKay, G. 2010. Use of incineration MSW Ash: A review. *Sustainability*, vol 2:7. P. 1943-1968. ISSN 2071-1050.

Li, J., Lu, H., Xu, Z. and Zhou, Y. 2008a. Critical rotational speed model of the rotating roll electrode in corona electrostatic separation for recycling waste printed circuit boards. *Journal of hazardous materials*, vol 154:1-3. P. 331-336. ISSN 0304-3894.

Li, J., Lu, H., Liu, S. and Xu, Z. 2008b. Optimizing the operating parameters of corona electrostatic separation for recycling waste scraped printed circuit boards by computer simulation of electric field. *Journal of hazardous materials*, vol 153:1-2. ISSN 0304-3894.

Li, J., Lu, H., Guo, J., Xu, Z. and Zhou, Z. 2007. Recycle technology for recovering resources and products from waste printed circuit boards. *Environmental science & technology*, vol 41:6. ISSN 0013-936X.

Mach, F., Adam, L., Kacerovský, J., Karban, P. and Doležel, I. 2014. Evolutionary algorithm-based multi-criteria optimization of triboelectrostatic separator. *Journal of Computational and Applied Mathematics*. ISSN 1110-757X.

Muchova, L., Bakker, E. and Rem, P. 2009. Precious metals in municipal solid waste incineration bottom ash. *Water, Air & Soil Pollution: Focus*, vol. 9:1-2. P. 107-116. ISSN 1567-7230.

PANalytical. 2011. Epsilon 3 käyttöopas. 2nd edition. Almelo, Netherlands: PANalytical B.V. 74 pages.

Boss, B. and Fredeen, J. 2004. *Concepts, Instrumentation and Techniques in Inductively Coupled Plasma Optical Emission Spectrometry*. 3rd edition. Shelton, USA: PerkinElmer. 120 pages.

Pöyry. 2012. Selvitys jätteen energiankäytöstä ja päästökaupasta. Työ- ja elinkeinoministeriö. [Web document]. [Referred 5.6.2014]. Available:

http://www.tem.fi/files/33506/Selvitys_jatteen_eneriakaytosta_ja_paastokaupasta_25.6.2012.pdf.

Retsch. 2014. Vibratory Disc Mill RS 200. [Web document]. [Referred 26.9.2014]. Available: <http://www.retsch.com/products/milling/disc-mills/rs-200/function-features/>.

Sabbas, T., Poletini, A., Pomi, R. et al. 2003. Management of municipal solid waste incineration residues. *Waste Management*, vol 23:1. P. 61-88. ISSN 0956-053X.

Steketee, J., Duzijn, R. and Born, J. 1997. Quality improvement of MSWI bottom ash by enhanced aging, washing and combination processes. *Studies in Environmental Science* 01/1997; DOI: 10.1016/S0166-1116(97)80184-7.

Tilmaline, A., Medles, K., Younes, M., Bendaoud, A. and Dascalescu, L. 2010. Roll-type versus free-fall electrostatic separation of tribocharged plastic particles. *IEEE Transactions on industry applications*, vol 46:4. P. 1564-1569. ISSN 0093-9994.

Tilmaline, A., Medels, K., Bendimerad, S., Boukholda, F. and Dascalescu, L. 2009. Electrostatic separators of particles: Application to plastic/metal, metal/metal and plastic/plastic mixtures. *Waste Management*, vol 29:1. P. 228-232. ISSN 0956-053X.

TiTan Metallurgical Services. 2014. Electrostatic Separation. [Web document]. [Referred 16.6.2014]. Available: <http://ttms999.com/electrostatic.html>.

US 7416145 B2. 2008. Rotor impact mill. Hall, D. and Wilde, T. US 11/424,833, 16.6.2006. Published 26.8.2008.

Vesanto, P. 2006. Jätteenpolton parhaan käytettävissä olevan tekniikan (BAT) vertailuasiakirjan käyttö suomalaisessa toimintaympäristössä. *Suomen ympäristö*, vol 27. ISSN 1796-1637.

Vlad, S., Urs, A., Iuga A. and Dascalescu, L. 2001. Premises for the numerical computation of conducting particle trajectories in plate-type electrostatic separators. *Journal of Electrostatics*, vol 51-52. P. 259-265. ISSN 0304-3886.

Vlad, S., Mihailescu, M., Ratifrou, D., Iuga, A. and Dascalescu, L. 2000a. Numerical analysis of the electric field in plate-type electrostatic separators. *Journal of Electrostatics*, vol 48:3-4. P. 217-229. ISSN 0304-3886.

Vlad, S., Iuga, A. and Dascalescu, L. 2000b. Modelling of conducting particle behavior in plate-type electrostatic separators. *Journal of Physics D: Applied Physics*, vol 33:2. P. 127-133. ISSN 1361-6463.

Waste control. 2014. Database of Waste Management Technologies. [Web document]. [Referred 27.5.2014]. Available: <http://www.epem.gr/waste-control/database/html/WtE-01.htm>.

Westenergy. 2014. Toimintaperiaate. [Web document]. [Referred 26.5.2014]. Available: <http://www.westenergy.fi/?l=fi&p=3&text=Toimintaperiaate>.

Wu, G., Li, J. and Xu, Z. 2013. Triboelectrostatic separation for granular plastic waste recycling: A review. *Waste Management*, vol 33:3. P. 585-597. ISSN 0956-053X.

Wu, J., Qin, Y., Zhou, Q and Xu, Z. 2009. Impact of nonconductive powder on electrostatic separation for recycling crushed waste printed circuit board. *Journal of Hazardous Materials*, vol 164:2-3. P. 1352-1358. ISSN 0304-3894.

Wu, J., Li, J. and Xu, Z. 2008. Optimization of key factors of the electrostatic separation for crushed PCB wastes using roll-type separator. *Journal of Hazardous Materials*, vol 154:1-3. P. 161-167. ISSN 0304-3894.

Xue, M., Yan, G., Li, J. and Xu, Z. 2012. Electrostatic separation for recycling conductors, semiconductors, and nonconductors from electronic waste. *Environmental Science and Technology*, vol 46:19. P. 10556-10563. ISSN 0013-936X.

Yang, Y., Xiao, Y., Voncken, J.H.L. and Wilson N. 2008. Thermal treatment and vitrification of boiler ash from a municipal solid waste incinerator. *Journal of Hazardous Materials*, vol. 154:1-3. P. 871-879. ISSN 0304-3894.